

Probe axion-like particles at the EIC in the coherent scattering

In collaboration with Reuven Balkin, Or Hen, Wenliang Li, Teng Ma, Yotam Soreq, Michael Williams

Hongkai Liu

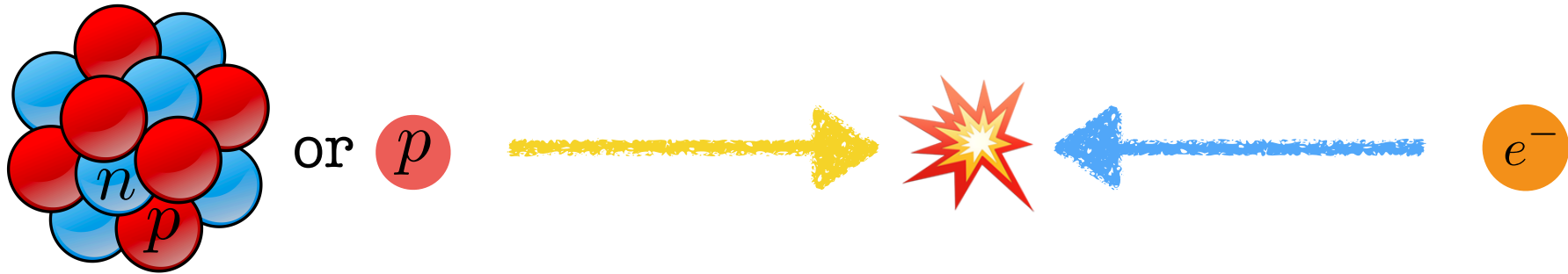


TECHNION

Israel Institute
of Technology

**Electroweak and Beyond the Standard Model Physics at the EIC
Feb. 12, 2024, Seattle**

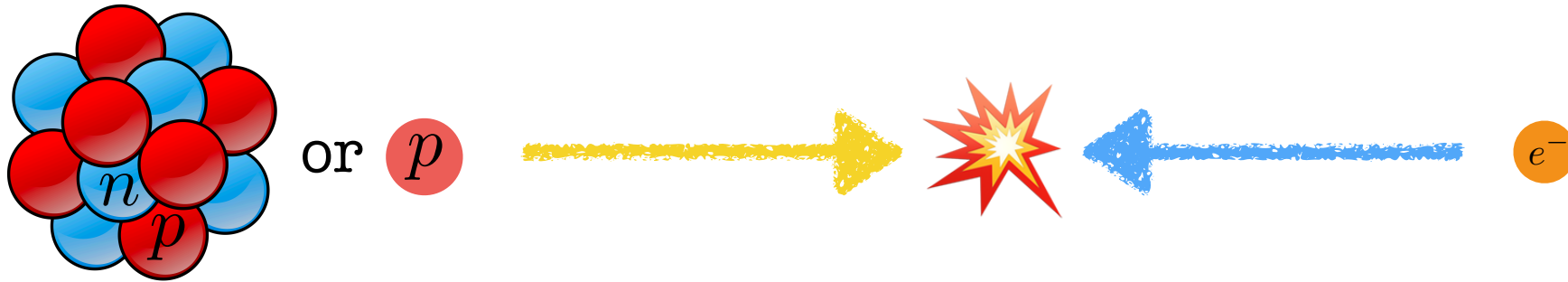
The Electron ion collider (EIC)



Understand quark-gluon structure of matter

- Understand the full three-dimensional momentum and spatial structure of nucleons and nuclei
- Understand the origin of nucleon mass and spin
- Study Nuclear PDFs
- ...

The Electron ion collider (EIC)

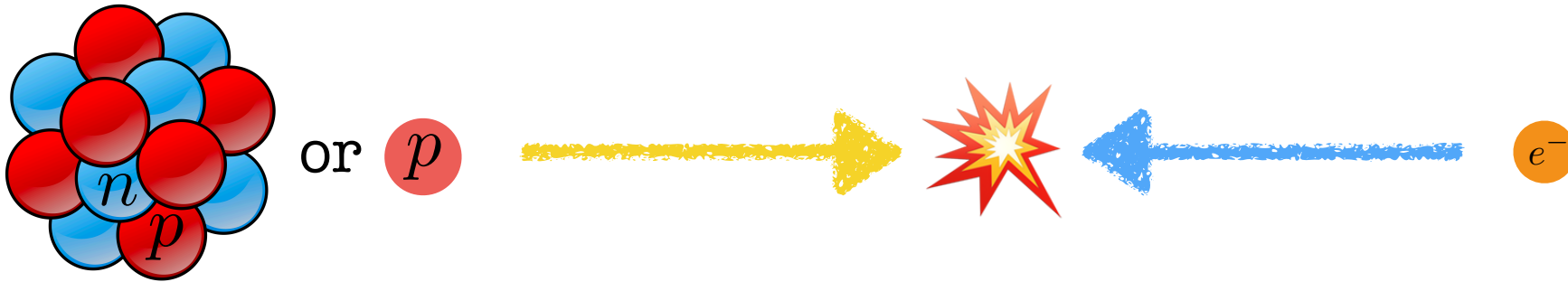


High energy:

E_e : up to 18 GeV

E_p : up to 275 GeV. For lead, $E_{\text{lead}} = 20$ TeV

The Electron ion collider (EIC)



High energy:

E_e : up to 18 GeV

E_p : up to 275 GeV. For lead, $E_{\text{lead}} = 20$ TeV

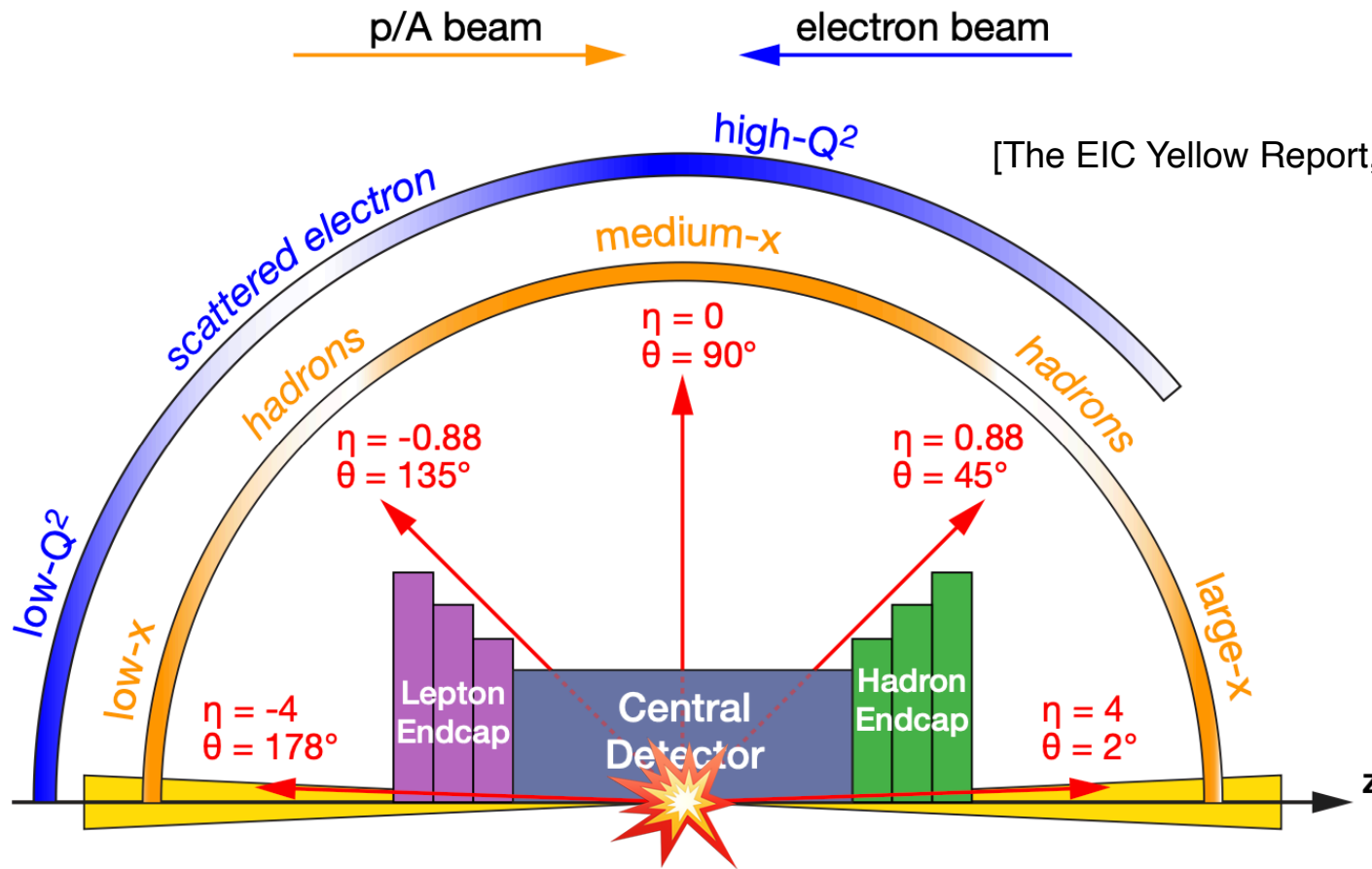
High luminosity:

$$L_{\text{peak}} = 10^{33} - 10^{34} \text{cm}^{-2} \text{s}^{-1}$$

- Most of its key physics topics are achievable with 10/fb
- The study of the spatial distributions of quarks and gluons in the proton requires 100/fb

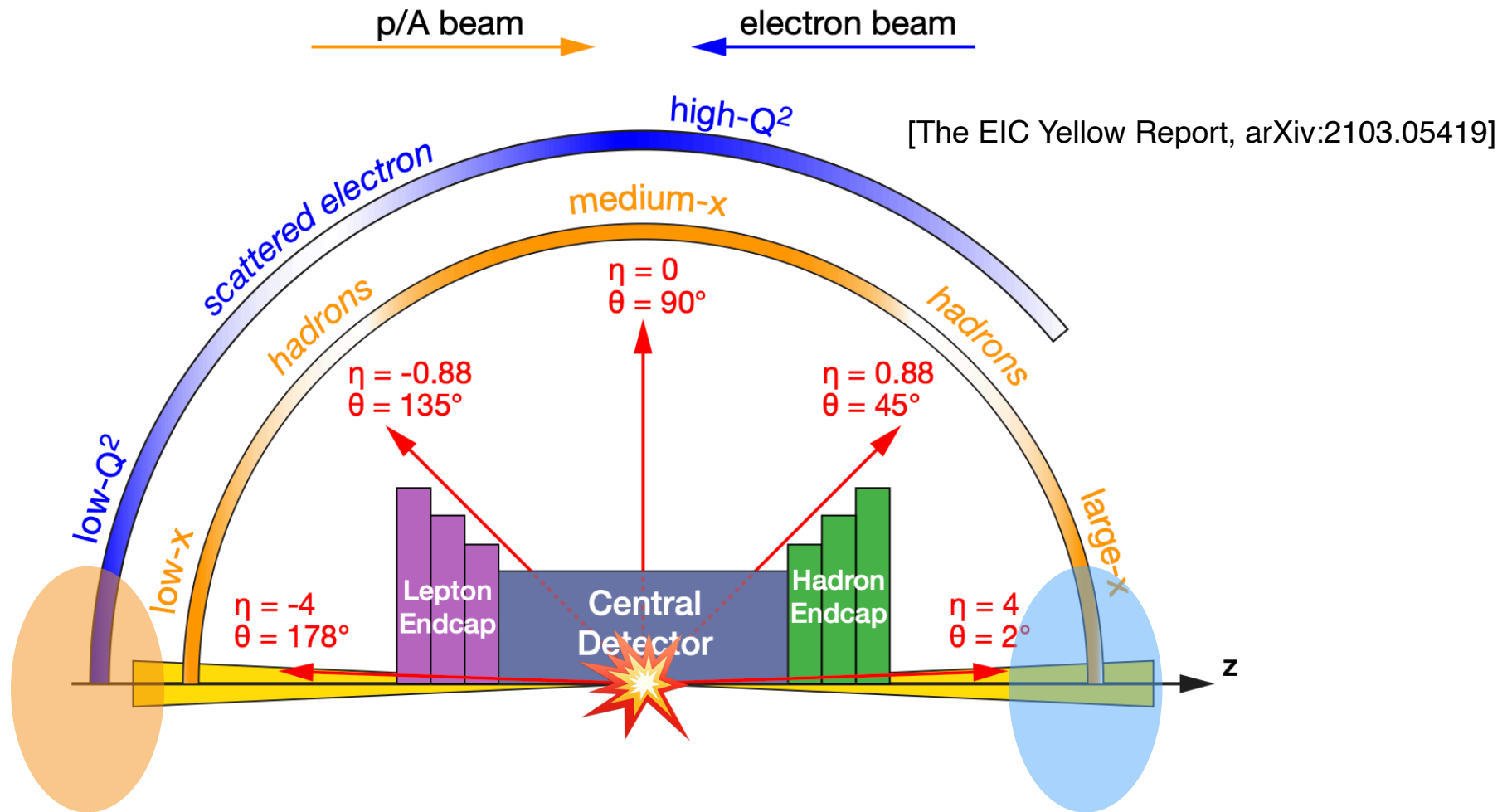
The Electron ion collider (EIC)

- The different detector systems observe different particle distributions.



The Electron ion collider (EIC)

- The different detector systems observe different particle distributions.



Far-backward detector:
Measure scattered electrons
with very low Q^2 and luminosity

Tagging recoiled electrons

[The EIC Yellow Report, arXiv:2103.05419]

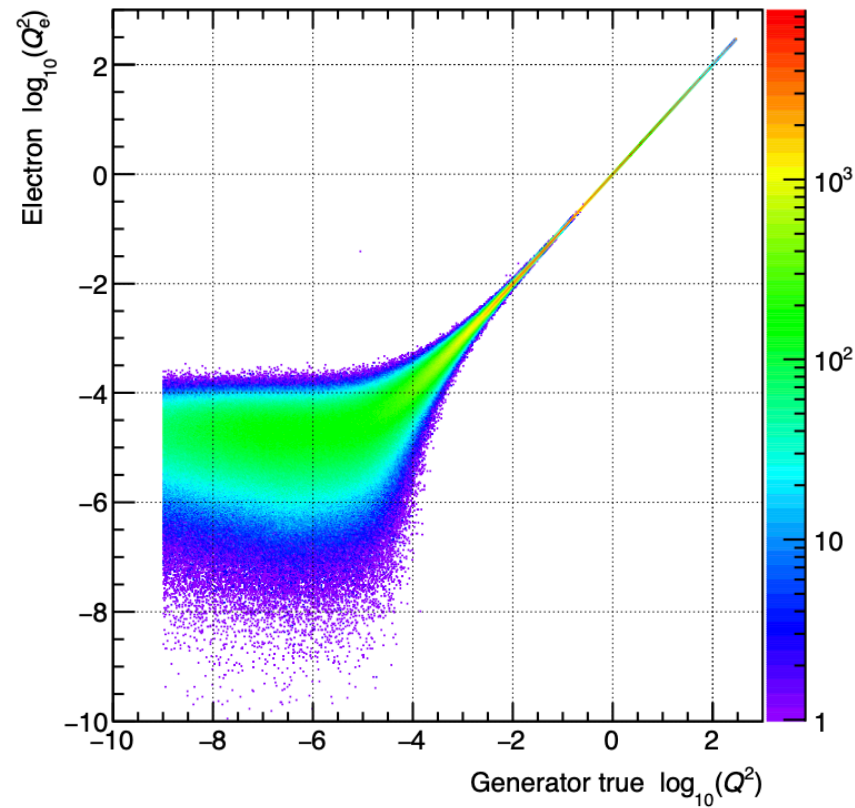


Figure 11.121: Comparison of generated and reconstructed electron Q_e^2 with smearing for beam angular divergence.

- Recoil electrons with very low- Q^2 (10^{-9} GeV^2) can be tagged.

Tagging recoiled electrons

[The EIC Yellow Report, arXiv:2103.05419]

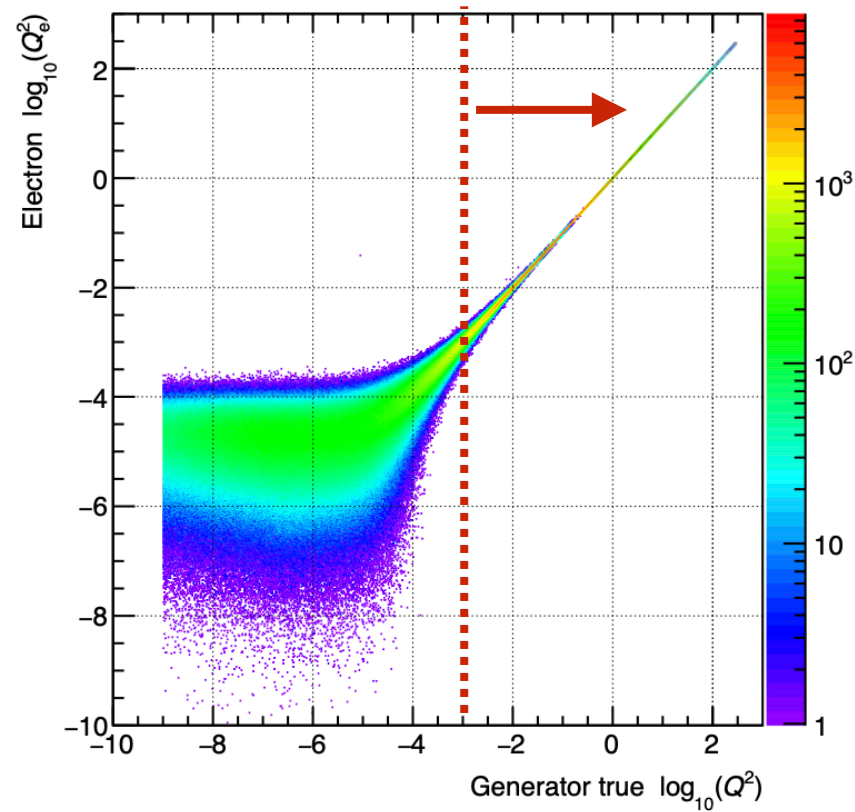
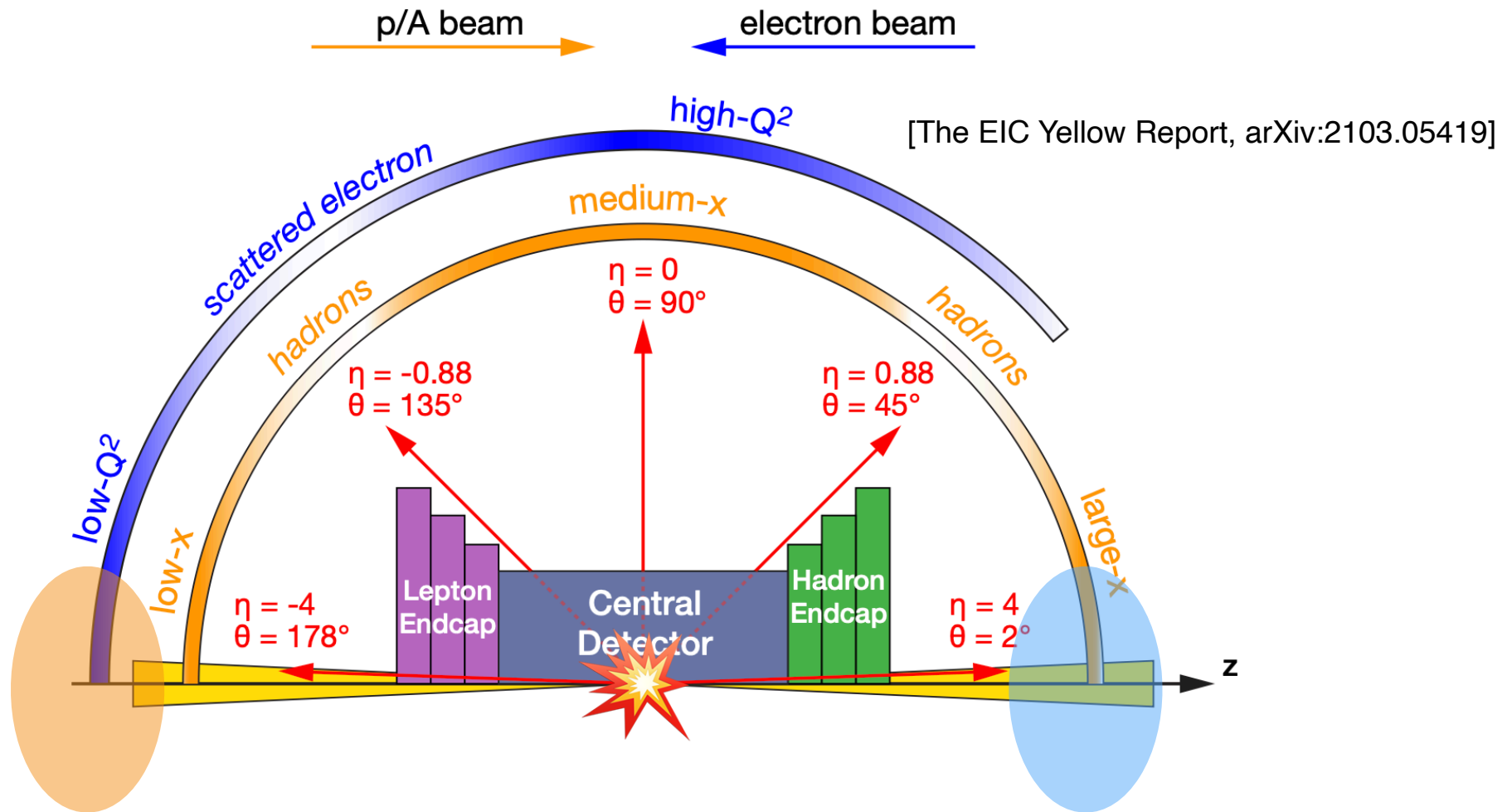


Figure 11.121: Comparison of generated and reconstructed electron Q_e^2 with smearing for beam angular divergence.

- Recoil electrons with very low- Q^2 (10^{-9} GeV^2) can be tagged.
- But only when $Q^2 > 10^{-3} \text{ GeV}^2$ we can have reasonable good resolution.

The Electron ion collider (EIC)

- The different detector systems observe different particle distributions.

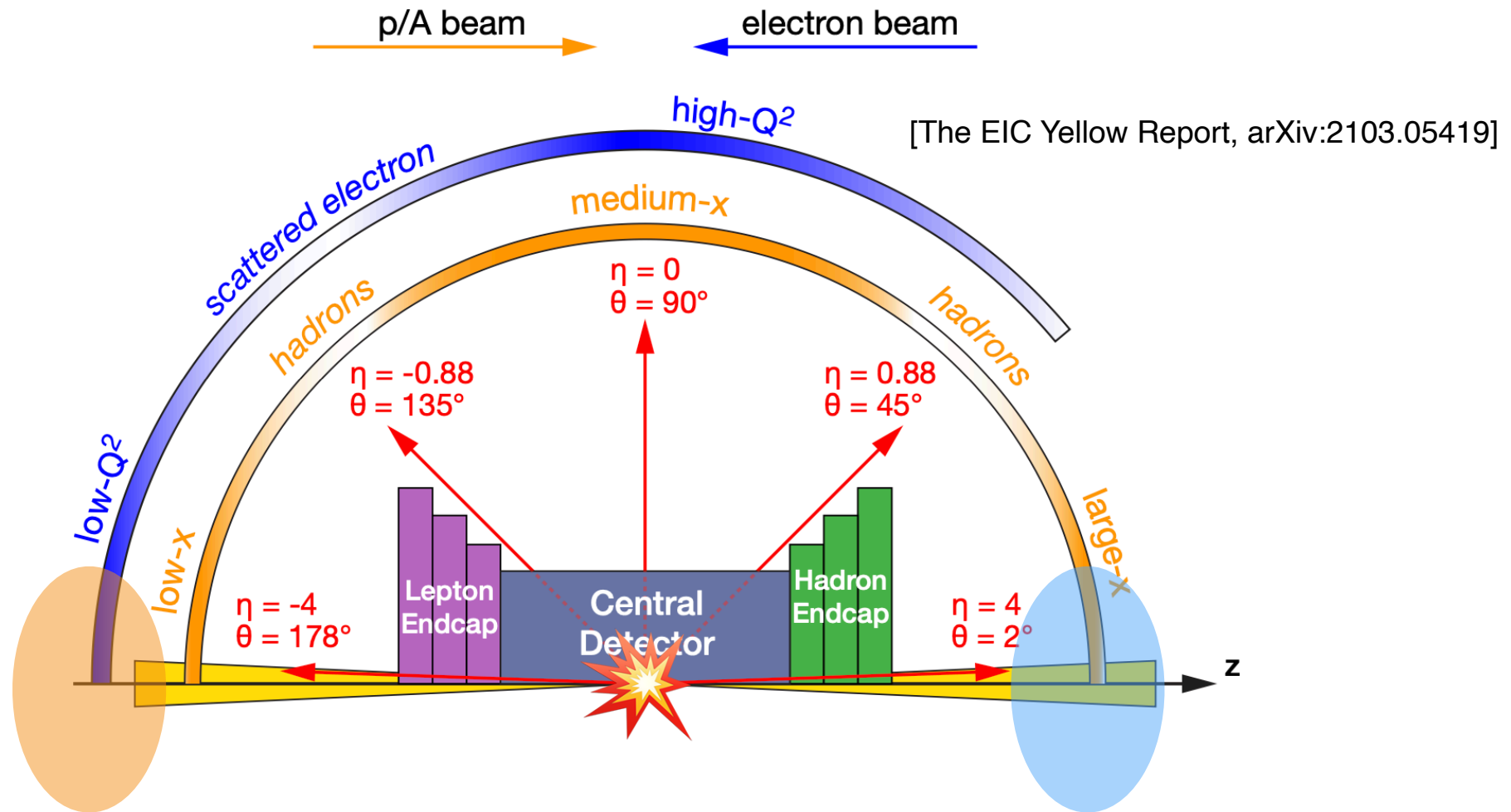


Far-backward detector:
Measure scattered electrons
with very low Q^2 and luminosity

Far-forward detector:
Can select the coherent collision
vetoing spectator neutrons from
nuclear breakup

The Electron ion collider (EIC)

- The different detector systems observe different particle distributions.



Far-backward detector:
Measure scattered electrons
with very low Q^2 and luminosity

Ideal for studying
coherent scattering

Far-forward detector:
Can select the coherent collision
vetoing spectator neutrons from
nuclear breakup

Motivation

$$\mathcal{L} = \mathcal{L}_{\text{SM}} + \mathcal{L}_{\nu \text{ mass}} + \mathcal{L}_{\text{DM}} + \mathcal{L}_{\text{BA}} + \mathcal{L}_{\text{strong CP}} + \dots$$

Motivation

$$\mathcal{L} = \mathcal{L}_{\text{SM}} + \mathcal{L}_{\nu \text{ mass}} + \mathcal{L}_{\text{DM}} + \mathcal{L}_{\text{BA}} + \mathcal{L}_{\text{strong CP}} + \dots$$



axion-like particle

Motivation

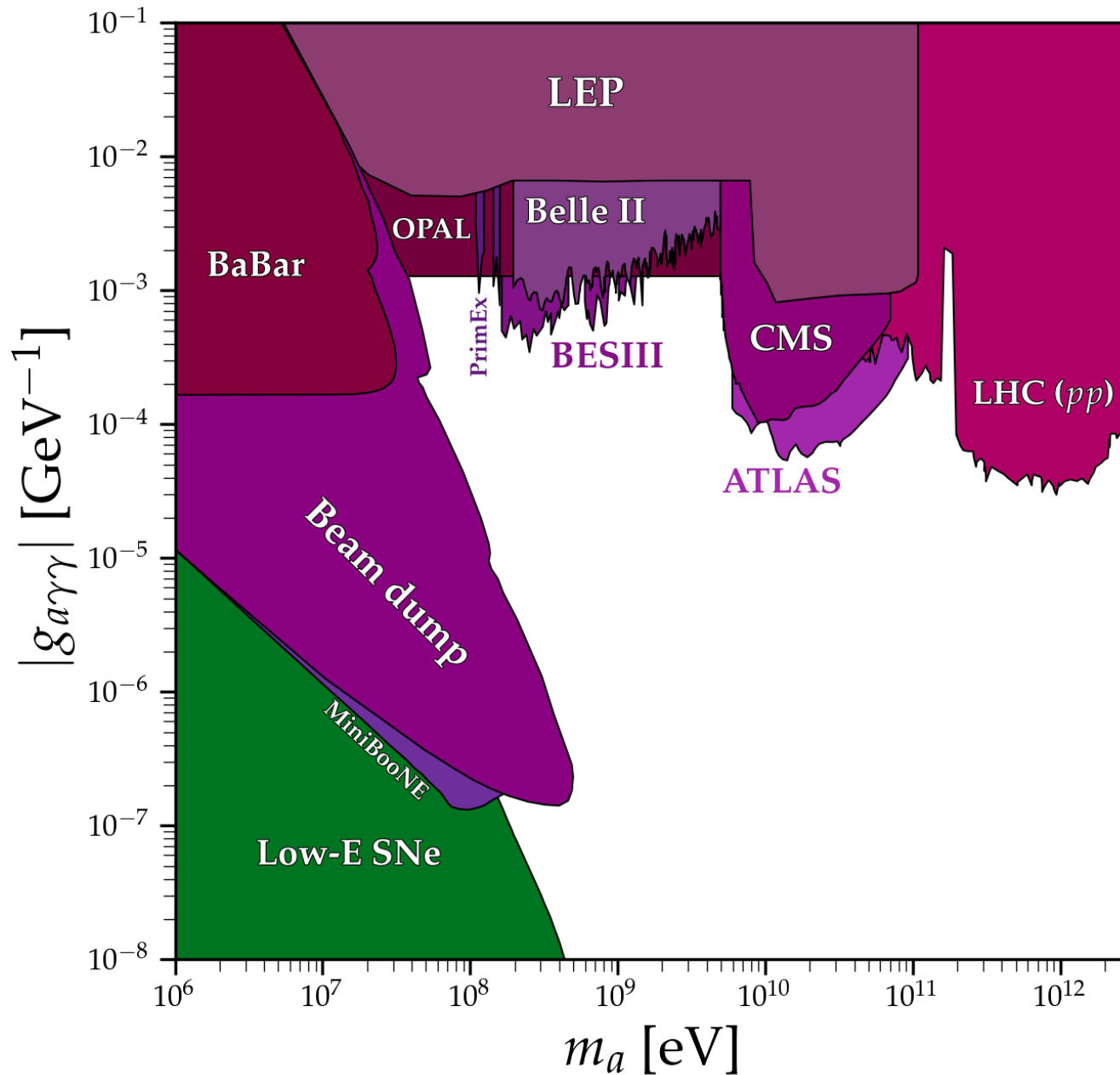
- QCD axion is a solution to the strong CP problem.

$$\mathcal{L}_a = \frac{1}{2}(\partial_\mu a)^2 - \frac{1}{2}m_a a^2 + \frac{a}{f_a} \frac{g_s^2}{32\pi^2} G\tilde{G}$$

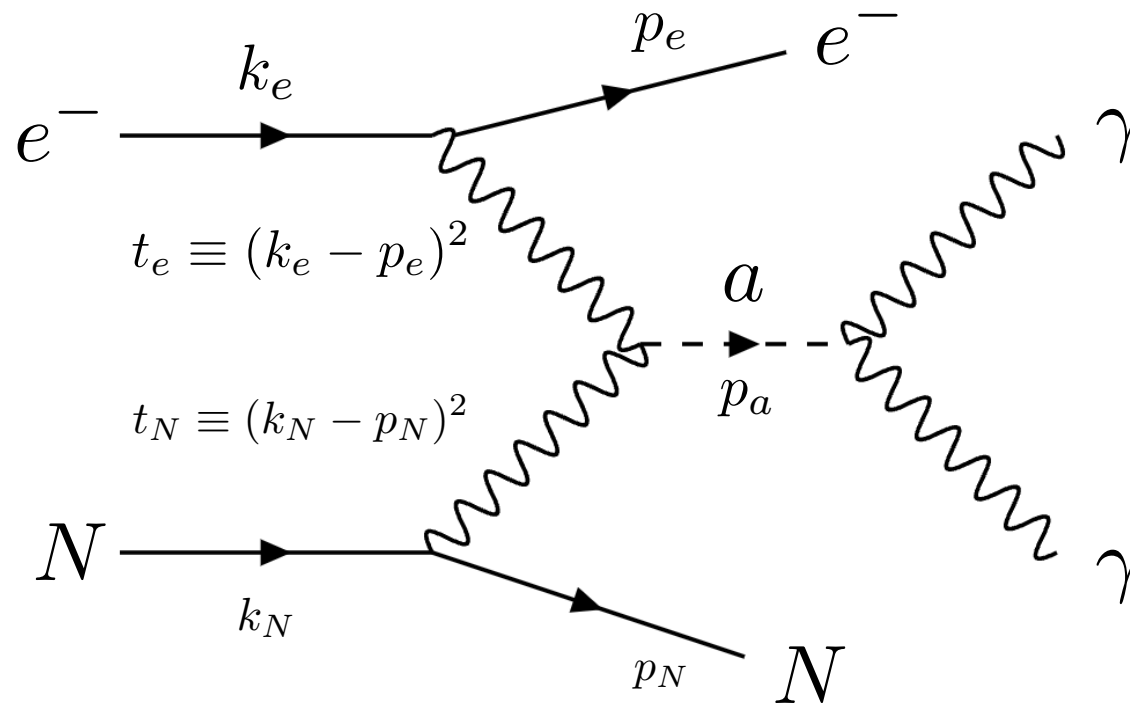
- In the simplest model, the relation between the axion mass and coupling are in a narrow band. However, in less minimum UV models, the mass-coupling relations can be shifted.
- To be UV independent, we adopt EFT description and treat the coupling and mass as two independent parameters \longrightarrow **axion-like particles (ALPs)**.
- Generally, ALPs are allowed to couple to both gauge bosons and fermions. Here, we only focus on investigating the **ALP-photon coupling** at the **electron-ion collider (EIC)**.

$$\mathcal{L}_a = \frac{1}{2}(\partial_\mu a)^2 - \frac{1}{2}m_a a^2 + \frac{a}{4\Lambda} F\tilde{F}$$

Current bounds



ALP coherent production at EIC



- Weakly coupled but with an enhancement of Z^2 in the ALP coherent production.
- The amplitude squared:

$$|\mathcal{M}_{2 \rightarrow 3}|^2 \propto (Z^2 e^4) / (t_e^2 t_N^2 \Lambda^2)$$

- As the recoil electron can be measured very precisely, the outgoing ion can be reconstructed:

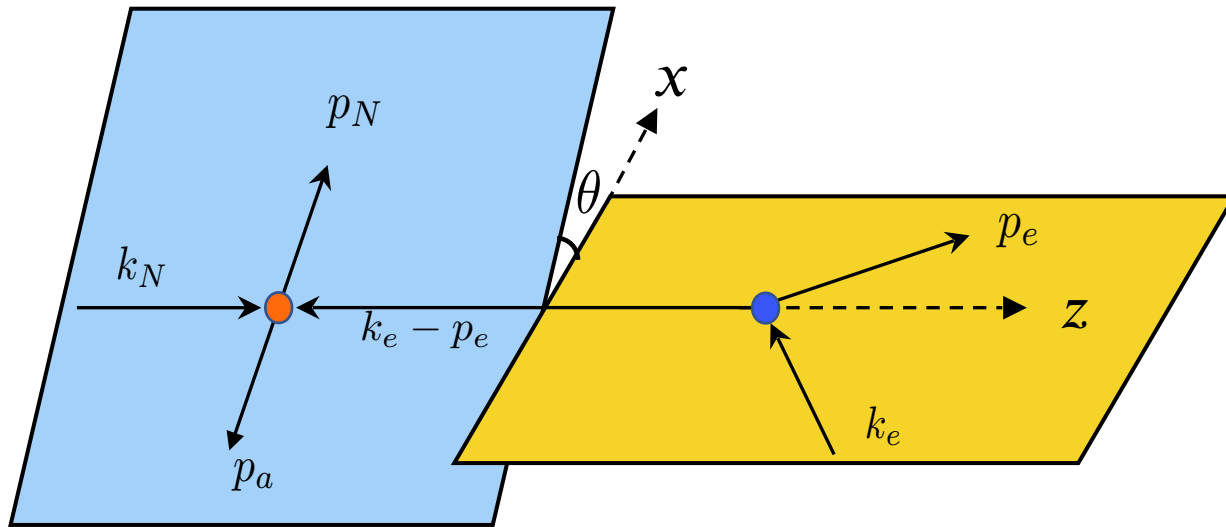
$$p_N^2 = (k_e + k_N - p_{\gamma_1} - p_{\gamma_2} - p_e)^2 = m_N^2$$

2-to-3 phase space

$$\Phi_3(s, m_e^2, m_N^2, m_a^2) = \int d^4 p_e d^4 p_N d^4 p_a \delta(p_e^2 - m_e^2) \delta(p_N^2 - m_N^2) \delta(p_a^2 - m_a^2) \\ \times \delta^4(k_e + k_N - p_e - p_N - p_a) \theta(p_e^0) \theta(p_N^0) \theta(p_a^0)$$

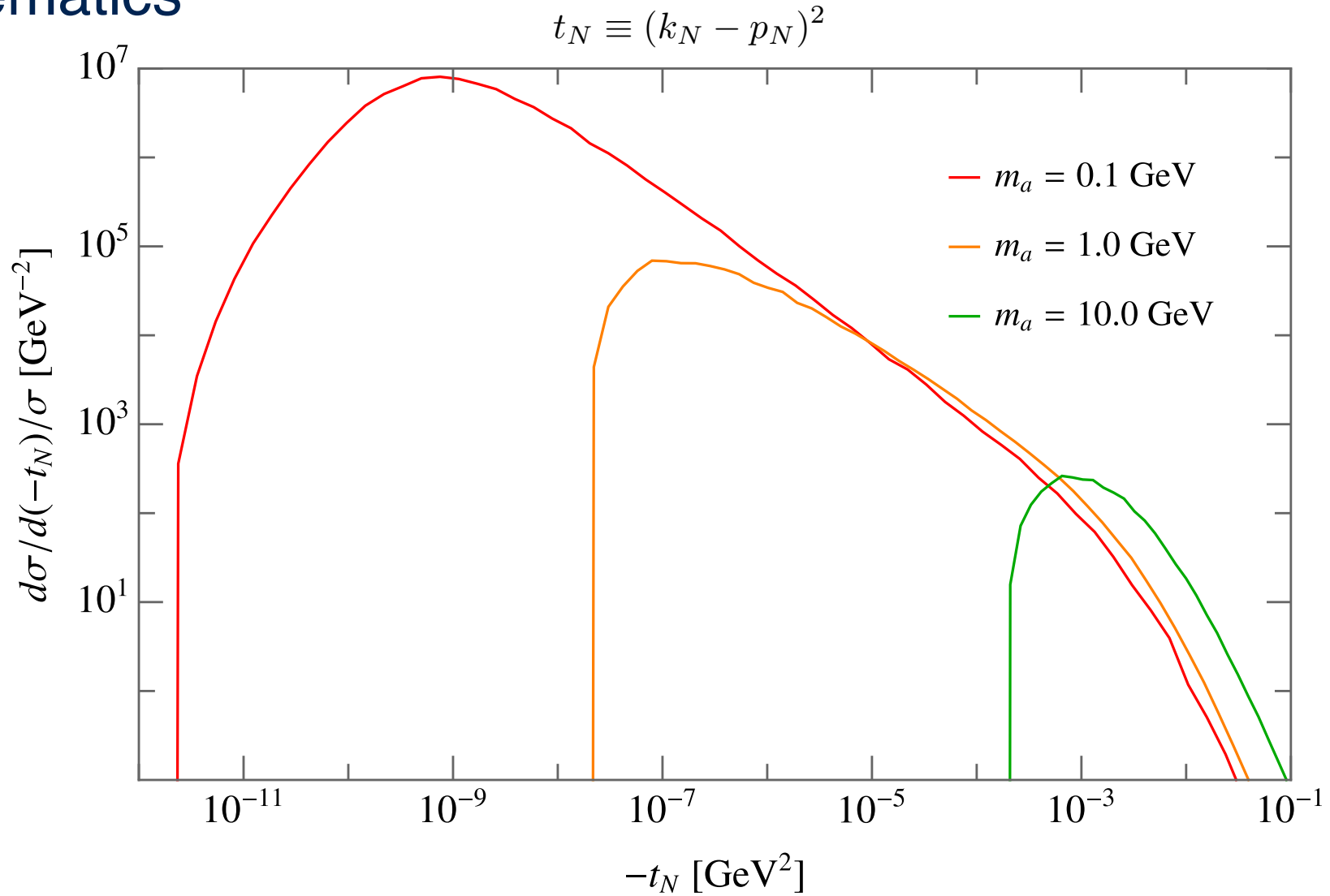
There are five independent kinematical variables. However, the integration over the azimuthal angle is trivial.

$$t_e \equiv (k_e - p_e)^2 \quad t_N \equiv (k_N - p_N)^2 \quad m_{aN}^2 \equiv (p_a + p_N)^2 \quad \cos \theta \equiv \frac{(\vec{k}_N \times \vec{p}_N) \cdot (\vec{k}_e \times \vec{p}_e)}{|\vec{k}_N \times \vec{p}_N| |\vec{k}_e \times \vec{p}_e|}$$



$$\frac{d\sigma_a^{2 \rightarrow 3}}{dt_e dt_N dm_{aN}^2 d\theta} = \frac{1}{(2\pi)^4} \frac{1}{4\sqrt{\lambda(s, m_e^2, m_N^2)}} \frac{1}{4\sqrt{\lambda(m_{aN}^2, m_N^2, t_e)}} \frac{1}{4[(k_e \cdot k_N)^2 - m_e^2 m_N^2]^{1/2}} |\mathcal{M}_a^{2 \rightarrow 3}|^2$$

Kinematics



$$(-t_N)_{\min} \approx 1.8 \times 10^{-8} \text{ GeV}^2 \left(\frac{m_a}{1.0 \text{ GeV}} \right)^4 \left(\frac{m_N}{193 \text{ GeV}} \right)^2 \left(\frac{\sqrt{s}}{1.2 \text{ TeV}} \right)^{-4}$$

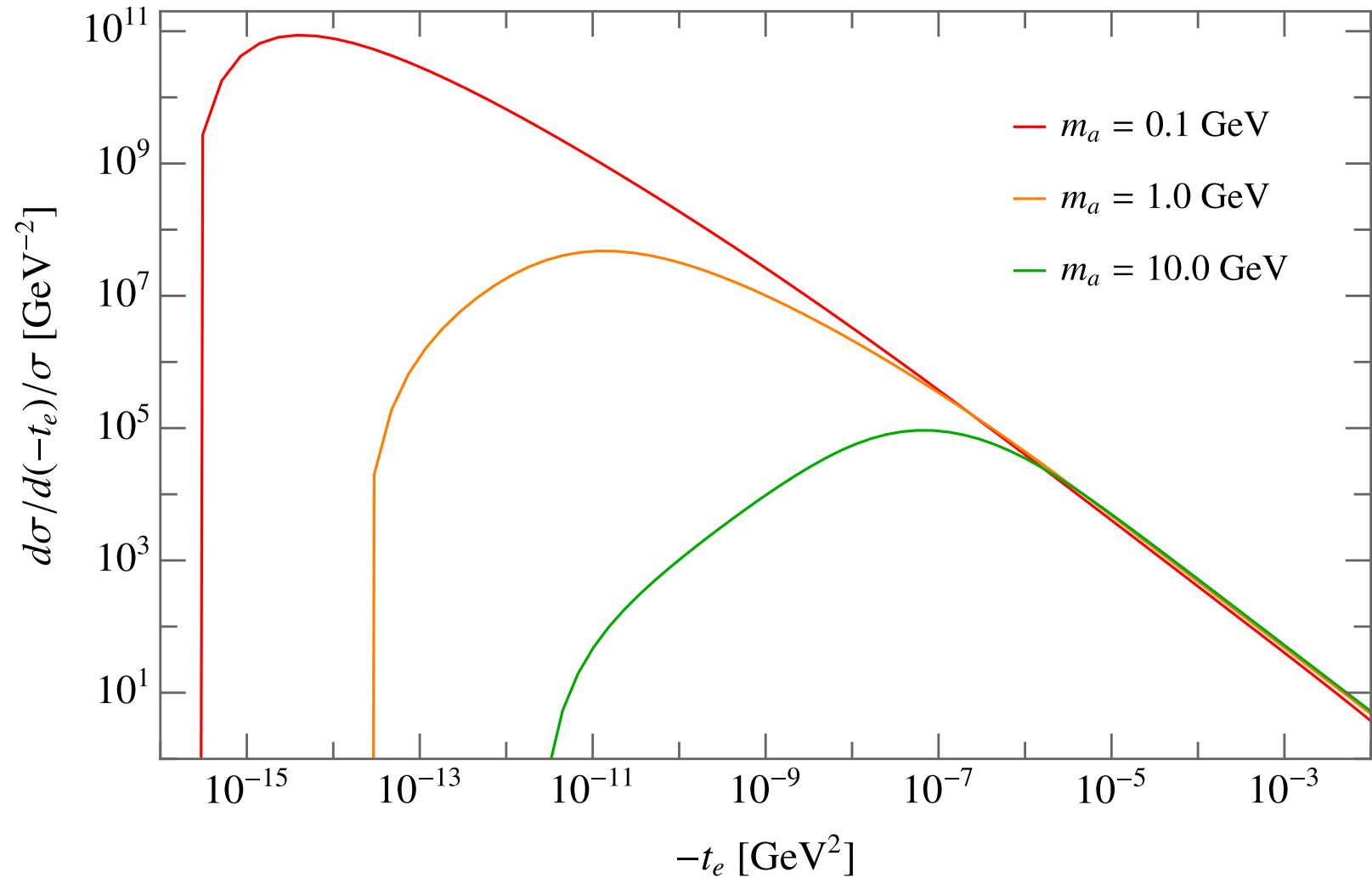
$$(-t_N)_{\min} \sim (1/r_N)^2 \sim 0.164A^{-2/3} \text{ GeV}^2$$



$$[m_a]_{\max} \sim 20 \text{ GeV} \left(\frac{E_e}{18 \text{ GeV}} \right)^{1/2} \left(\frac{E_N/A}{100 \text{ GeV}} \right)^{1/2} \left(\frac{A}{207} \right)^{-1/6}$$

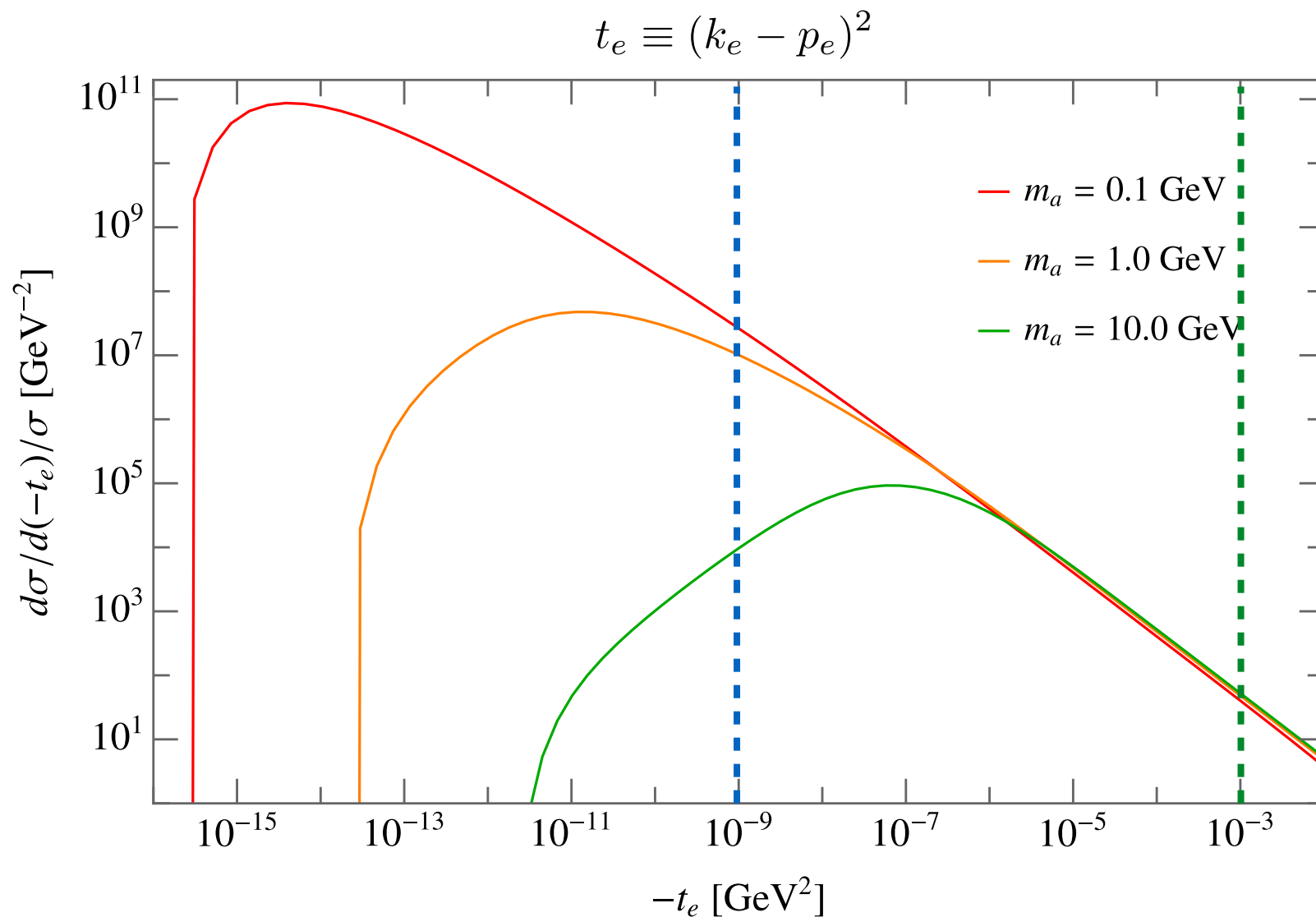
Kinematics

$$t_e \equiv (k_e - p_e)^2$$



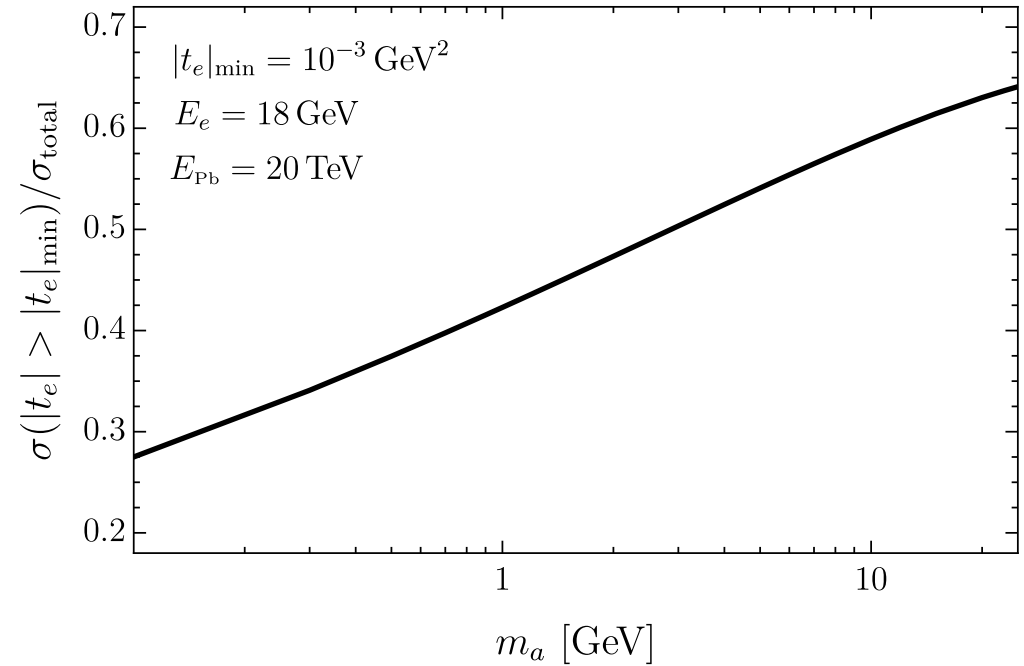
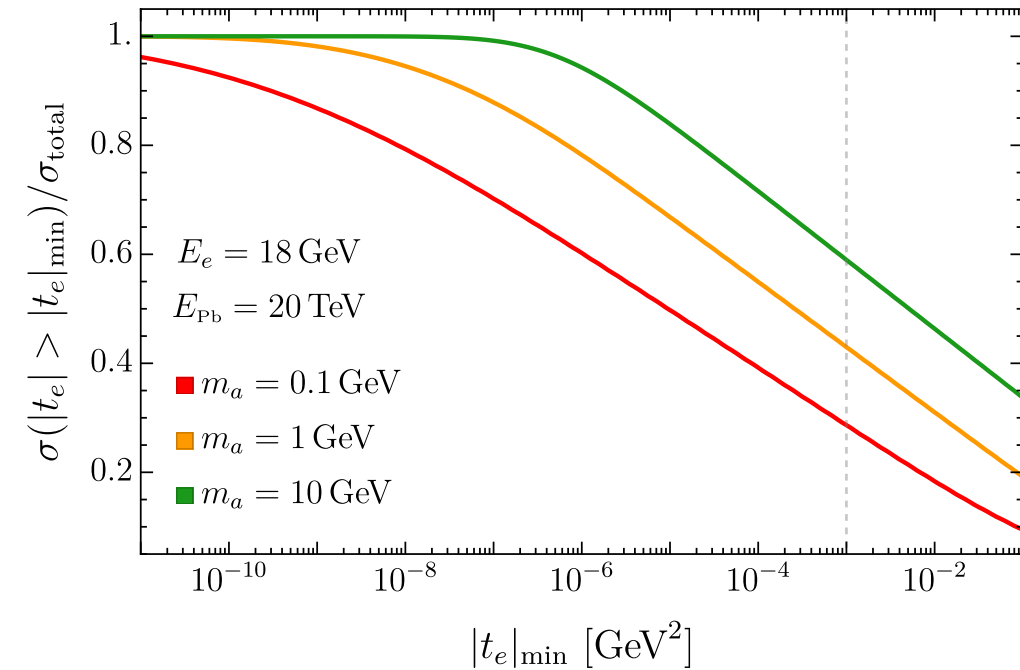
$$(-t_e)_{\min} \approx 1.9 \times 10^{-14} \text{ GeV}^2 \left(\frac{m_a}{1.0 \text{ GeV}} \right)^2 \left(\frac{m_N}{193 \text{ GeV}} \right)^2 \left(\frac{\sqrt{s}}{1.2 \text{ TeV}} \right)^{-4}$$

Kinematics



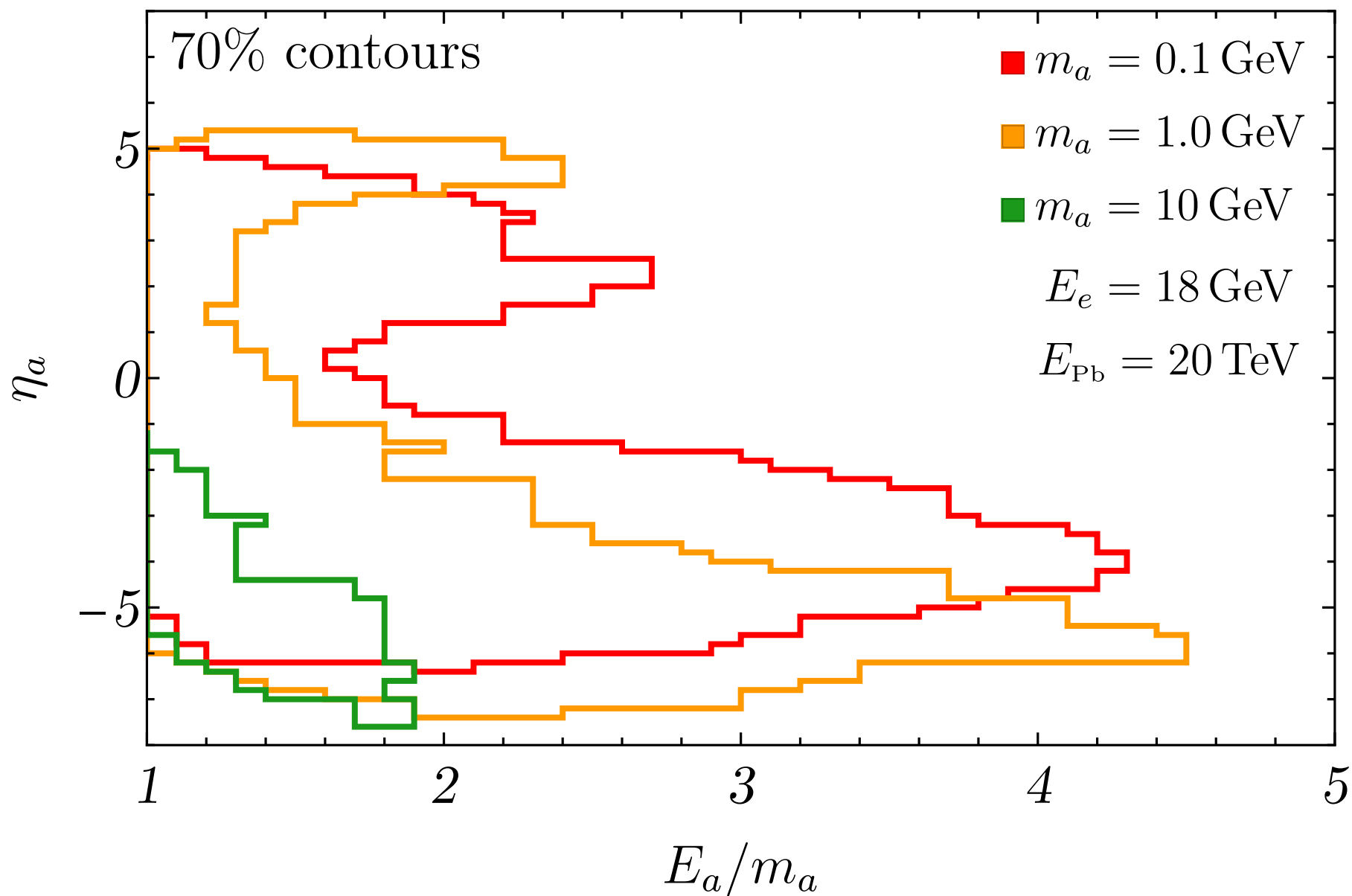
$$(-t_e)_{\min} \approx 1.9 \times 10^{-14} \text{ GeV}^2 \left(\frac{m_a}{1.0 \text{ GeV}} \right)^2 \left(\frac{m_N}{193 \text{ GeV}} \right)^2 \left(\frac{\sqrt{s}}{1.2 \text{ TeV}} \right)^{-4}$$

Tagging recoiled electrons

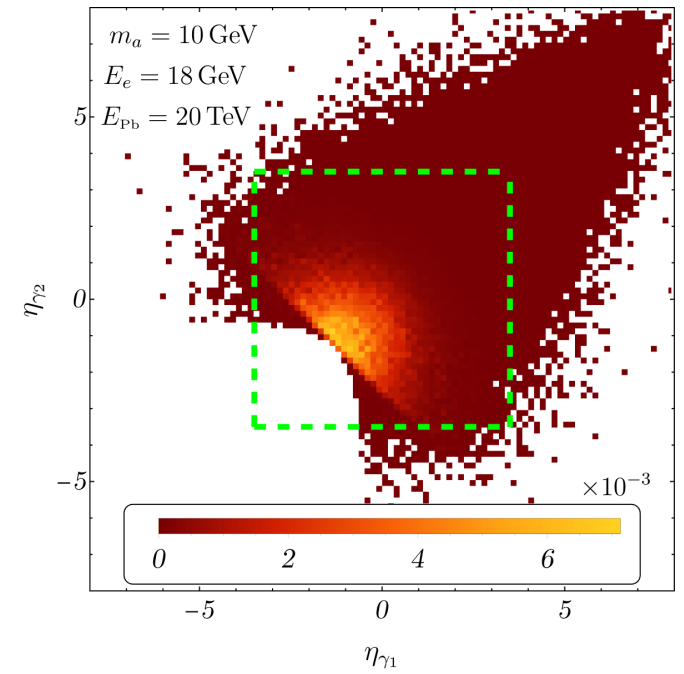
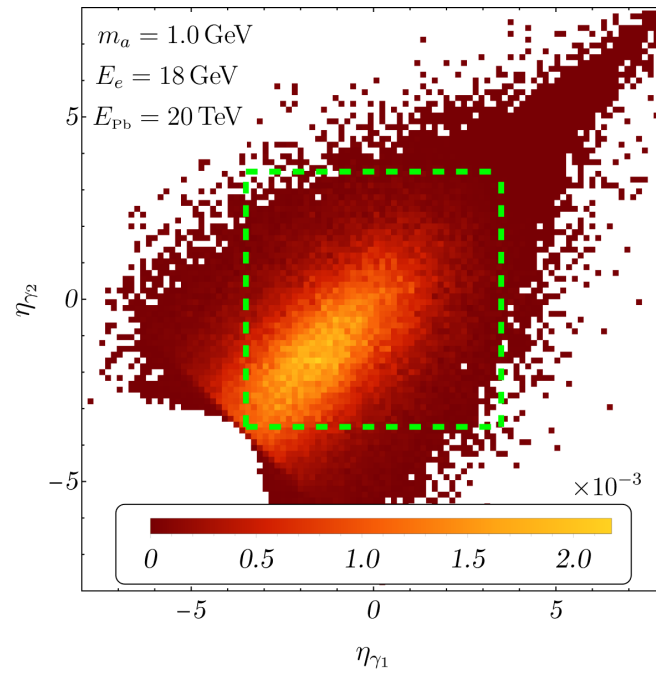
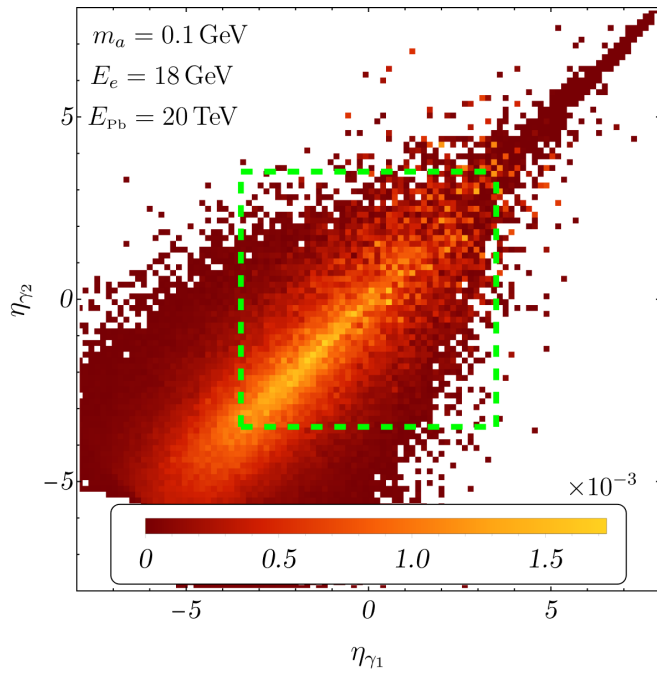


- We require $-t_e > 10^{-3}$ GeV² to have reasonable good resolution.
- The efficiencies is around 40% for 1 GeV ALP.

Kinematics



Kinematics



Prompt searches:

- The signal is clean:

$$2\gamma + \text{recoil } e^- + \text{intact lead ion}$$

- Basic cuts:

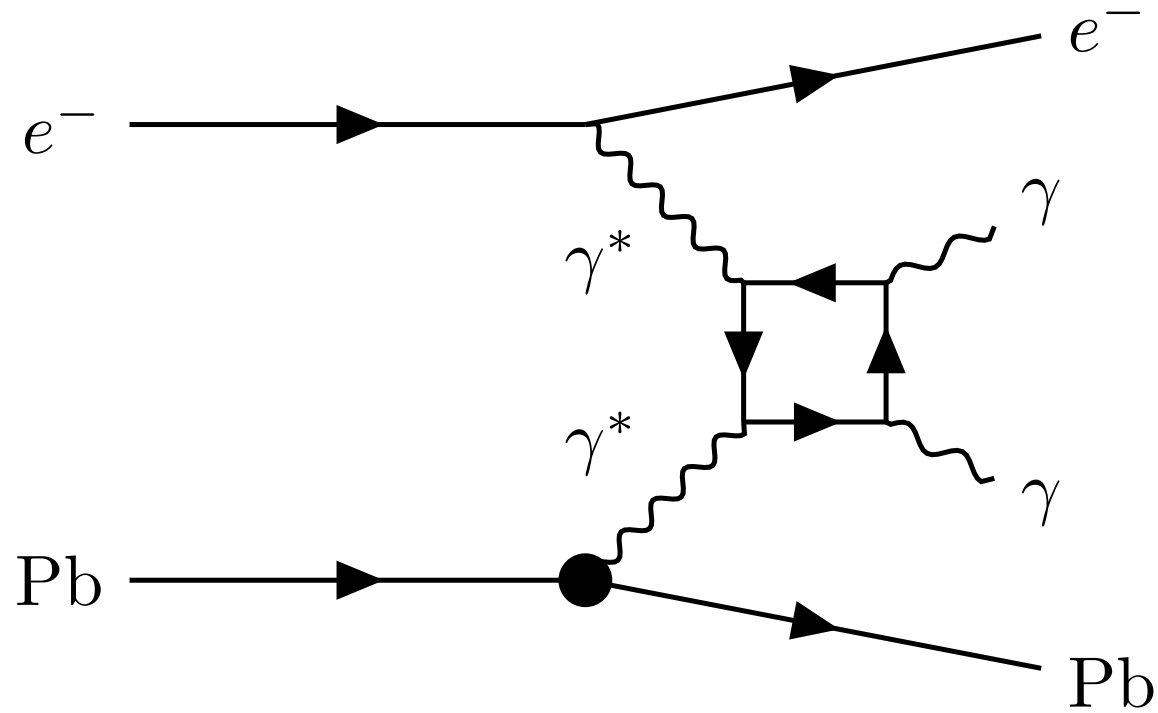
- Due to the angular acceptance, we require $|\eta_\gamma| < 3.5$
- To ensure an excellent photon resolution and suppress beam related background, we require $E_\gamma > 1 \text{ GeV}$
- Perform a resonance search in the invariant mass of two photons

$$m_{\gamma\gamma} \in [m_a - 2\Delta m_{\gamma\gamma}, m_a + 2\Delta m_{\gamma\gamma}]$$

- From a simulation:

$m_{\gamma\gamma} [\text{GeV}]$	0.3	0.5	0.7	0.9	2.0	4.0	7.0	15.0
$\Delta m_{\gamma\gamma}/m_{\gamma\gamma} (\%)$	3.5	3.3	3.1	2.8	1.7	1.2	0.97	0.72

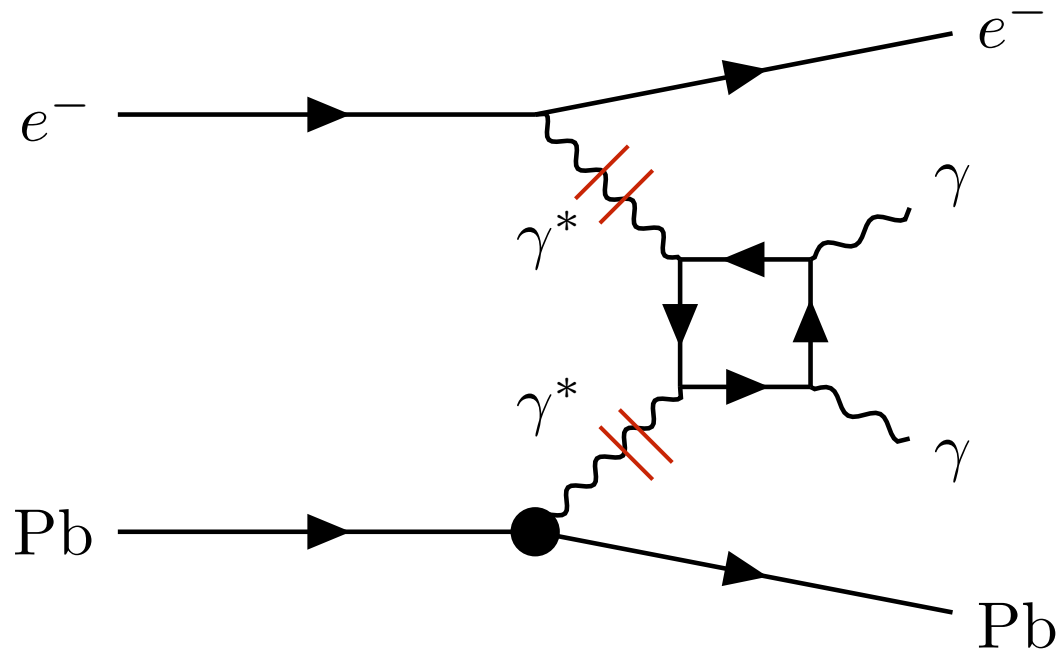
Backgrounds: light-by-light scattering



• **Irreducible** light-by-light (LBL) scattering: $\gamma + \gamma \rightarrow \gamma + \gamma$

• We use the equivalent photon approximation (EPA) to estimate the backgrounds

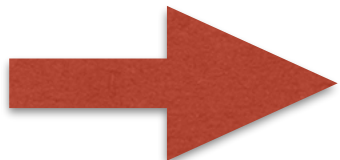
EPA



$$\frac{d\sigma_{eN \rightarrow eNX}}{d\hat{s}}(\hat{s}) = \frac{1}{\hat{s}} \int_{\frac{\hat{s}}{4E_{pb}}}^{E_e} \frac{d\omega_1}{\omega_1} f_{\gamma/e}(\omega_1) f_{\gamma/N}(\omega_2) \hat{\sigma}_{\gamma\gamma \rightarrow X}(\hat{s})$$

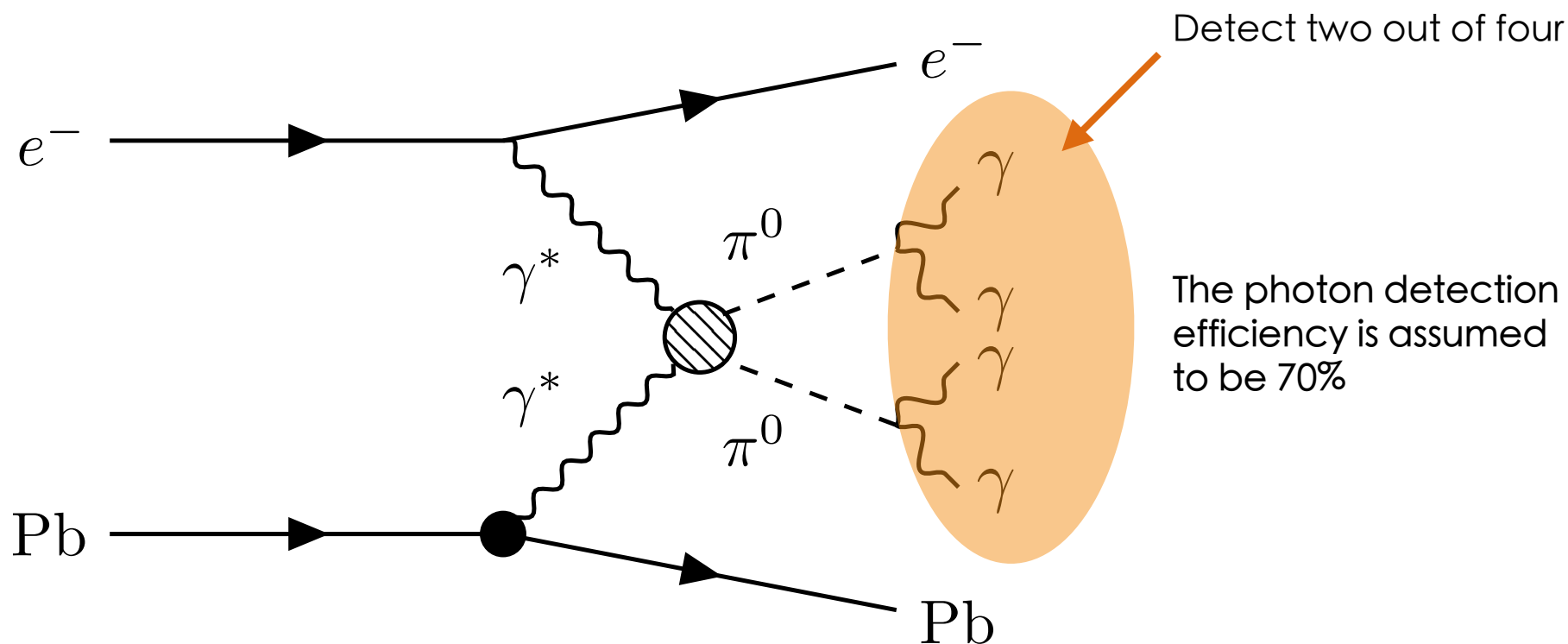
• LBL scattering: $\hat{\sigma}_{\gamma\gamma \rightarrow \gamma\gamma}(\hat{s}) \sim \frac{10^{-6}}{\hat{s}}$ [Bern, Freitas, Dixon, Ghinculov, Wong, hep-ph/0109079]

• Signal: $\hat{\sigma}_{\gamma\gamma \rightarrow a \rightarrow \gamma\gamma}(\hat{s}) = \frac{\pi m_a^2}{8\Lambda^2} \delta(\hat{s} - m_a^2)$



$$\frac{\sigma_a}{\sigma_{\text{LBL}}} \approx 20 \left(\frac{\text{TeV}}{\Lambda} \right)^2 \left(\frac{m_{\gamma\gamma}}{2 \text{ GeV}} \right)^2 \left(\frac{0.01}{\Delta m_{\gamma\gamma}/m_{\gamma\gamma}} \right)$$

Backgrounds: pion-pair production



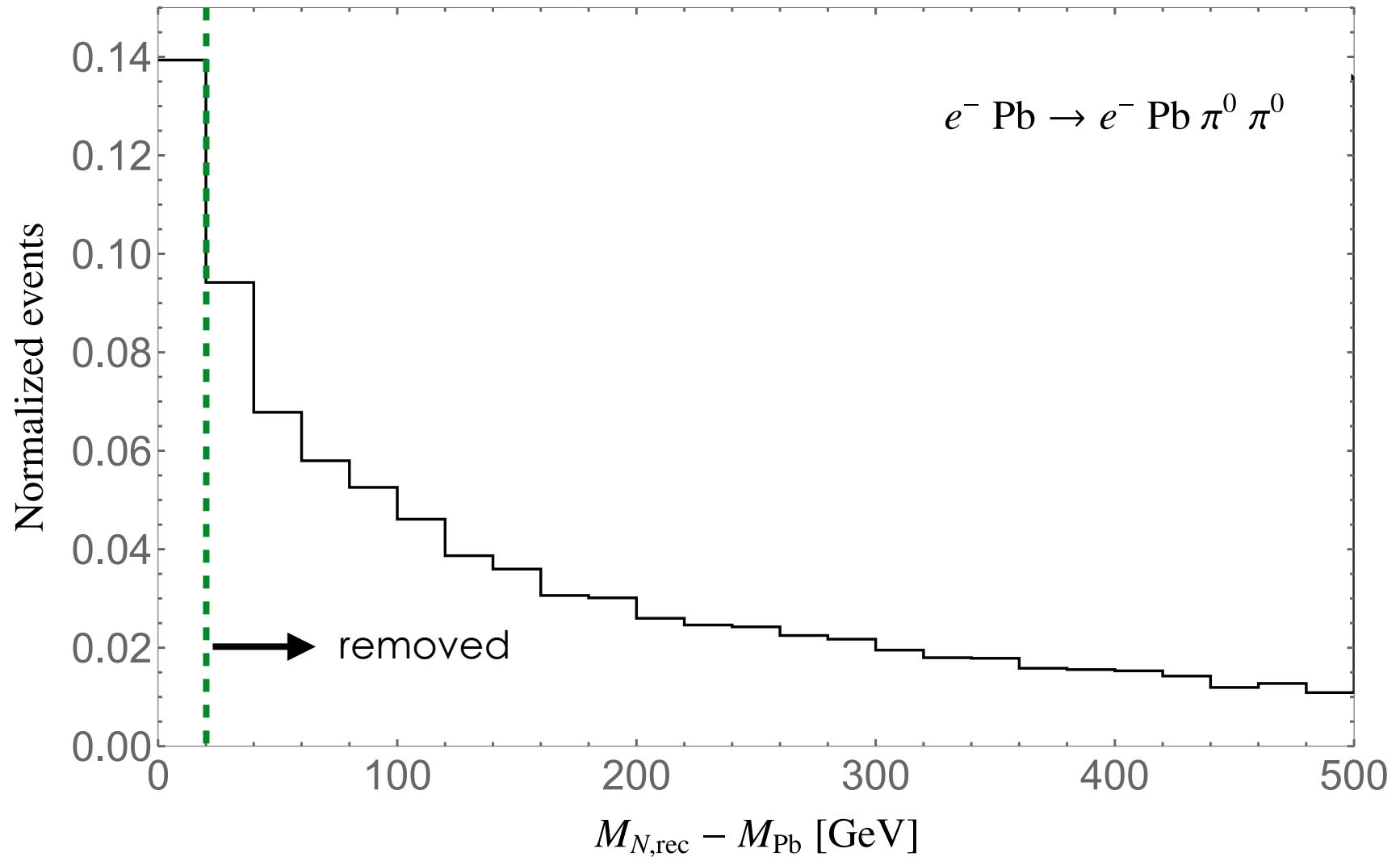
- **Reducible** Pion-pair production $\gamma + \gamma \rightarrow \pi^0 + \pi^0 \rightarrow 4\gamma$

Several processes contribute to the neutral pion pair production

[Klusek-Gawenda, Szczurek, arXiv:1302.4204]

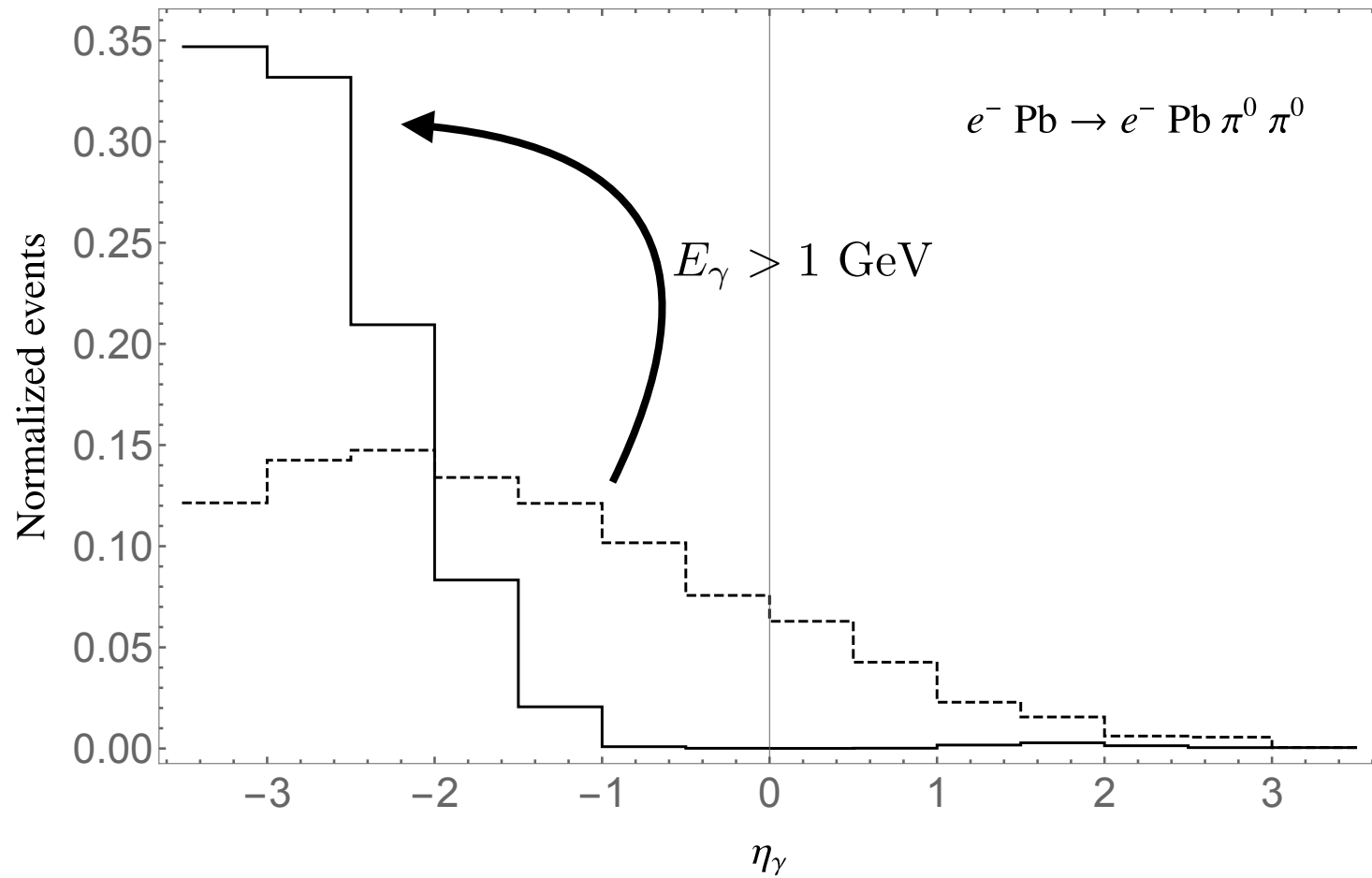
Miss two photons: $p_N^{\text{rec},2} = (p_N^{\text{true}} + p_{\gamma_1}^{\text{miss}} + p_{\gamma_2}^{\text{miss}}) > m_N^2$

Backgrounds: pion-pair production



Require: $M_{\text{Pb,rec}} - M_{\text{pb}} \leq 10\% M_{\text{Pb}}$ $|\Delta\phi_{\gamma\gamma} - \pi| < 0.2$

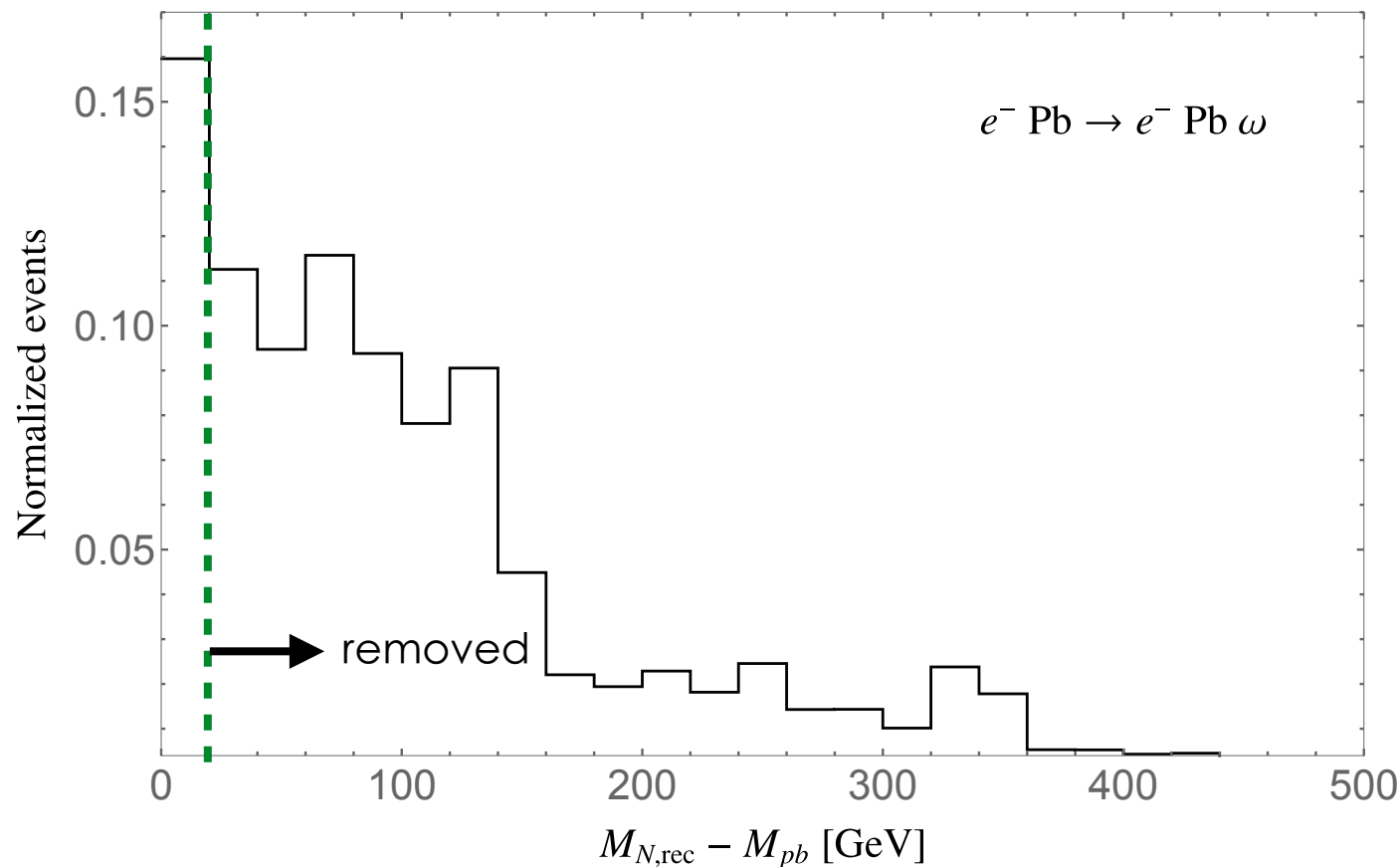
Backgrounds: pion-pair production



Backgrounds: omega production

Detect two out of three

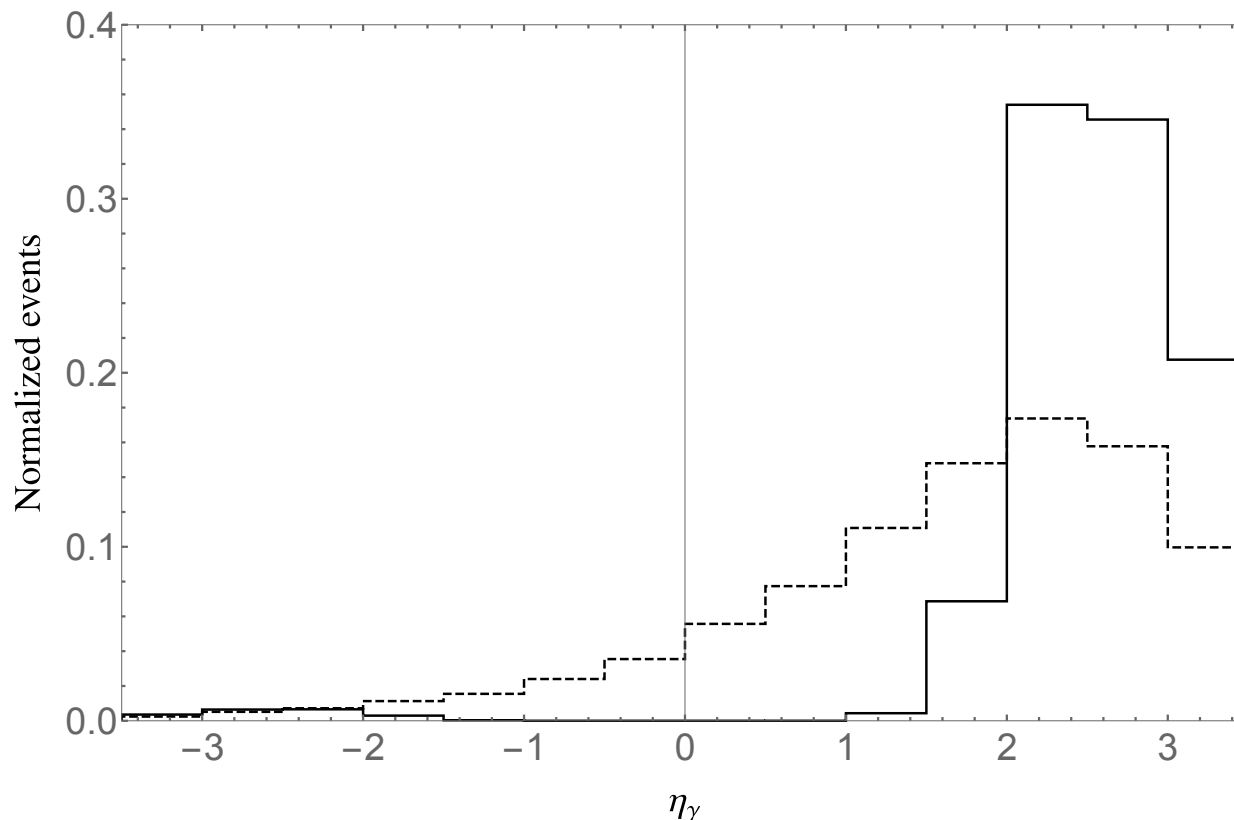
- **Reducible** $\omega(782) : \gamma + N \rightarrow \omega + N, \omega \rightarrow \pi^0 + \gamma \rightarrow 3\gamma$
- Only contribute at $m_{\gamma\gamma} < m_\omega$
- We take the photoproduction of omega resonance from [\[Ballam, etc, PRD 7 \(1973\) 3150\]](#)



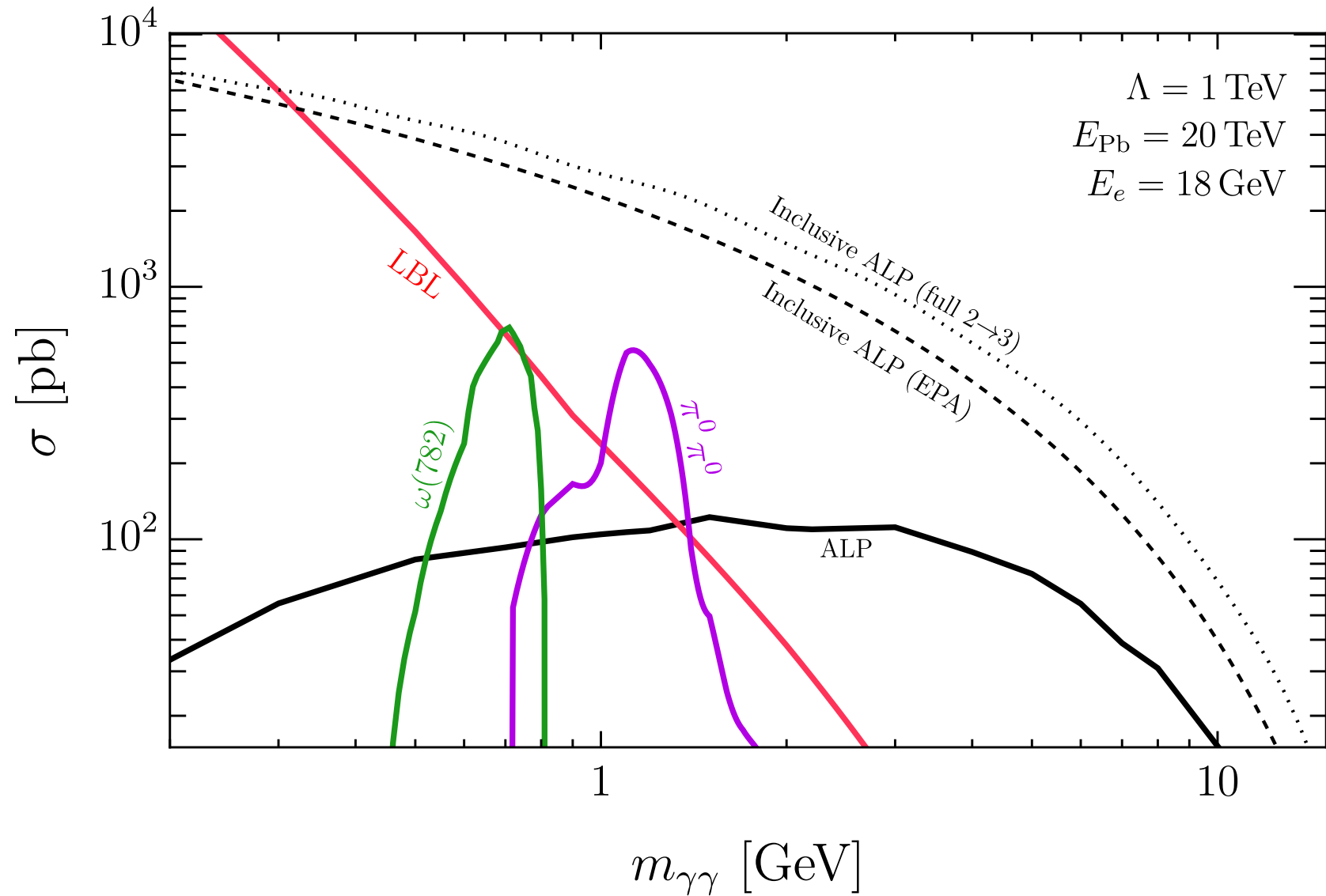
Backgrounds: omega production

Detect two out of three

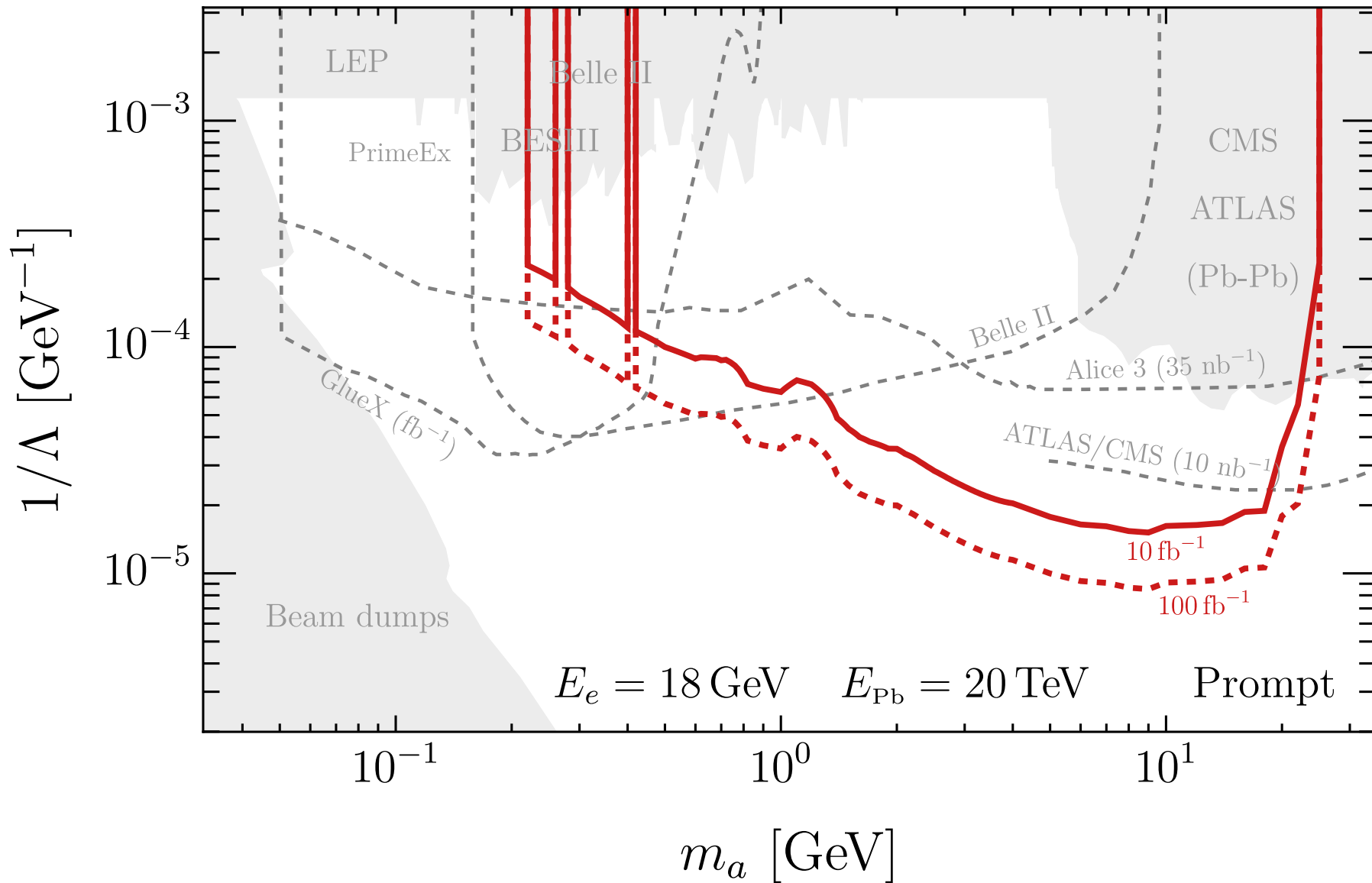
- **Reducible** $\omega (782) : \gamma + N \rightarrow \omega + N, \omega \rightarrow \pi^0 + \gamma \rightarrow 3\gamma$
- Only contribute at $m_{\gamma\gamma} < m_\omega$
- We take the photoproduction of omega resonance from [\[Ballam, etc, PRD 7 \(1973\) 3150\]](#)
- Further require $\eta_{\gamma_{1,2}} < 0$ if $m_{\gamma\gamma} < m_\omega$



Cross sections after the cuts



EIC projections: prompt searches



EIC projections: displaced-vertex searches

ALP decay width $\Gamma_a = \frac{m_a^3}{64\pi\Lambda^2}$

ALP decay length at the lab frame $L_a \equiv \frac{\beta\gamma}{\Gamma_a}$

ALP decay probability between distance L_R and L_{EM} is

$$\mathcal{P}(L_R, L_{\text{EM}}) = \exp\left(-\frac{L_R}{L_a}\right) - \exp\left(-\frac{L_{\text{EM}}}{L_a}\right)$$

L_R is the spatial resolution of di-photon vertex

L_{EM} is the size of the EM calorimeter

Consider 3 scenarios: $(L_R, L_{\text{EM}}) = (10, 100), (50, 100), (75, 150)$ cm

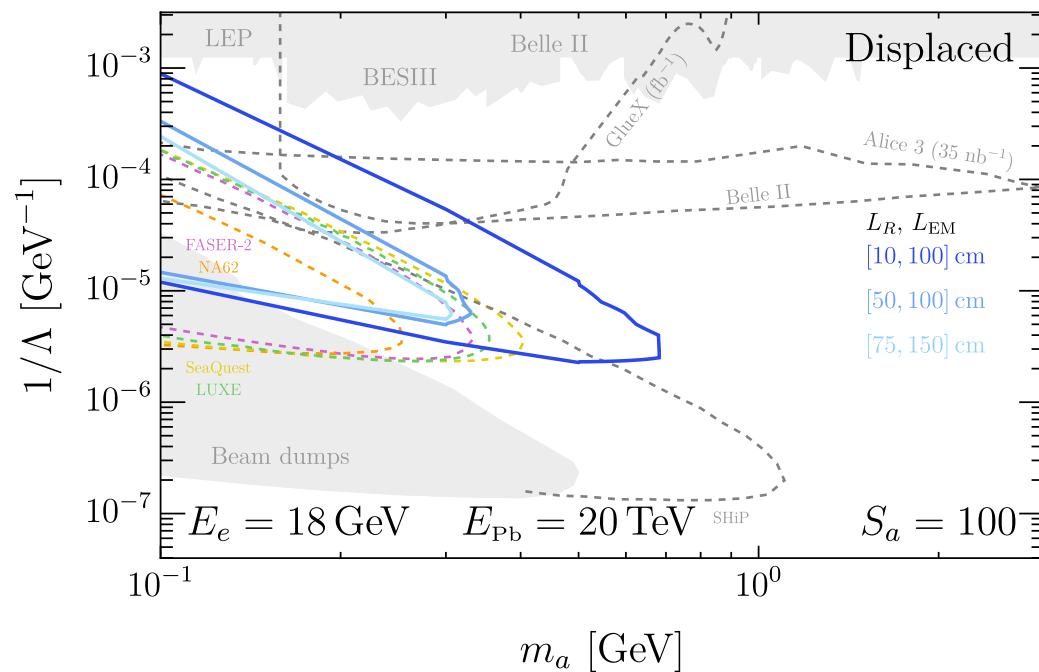
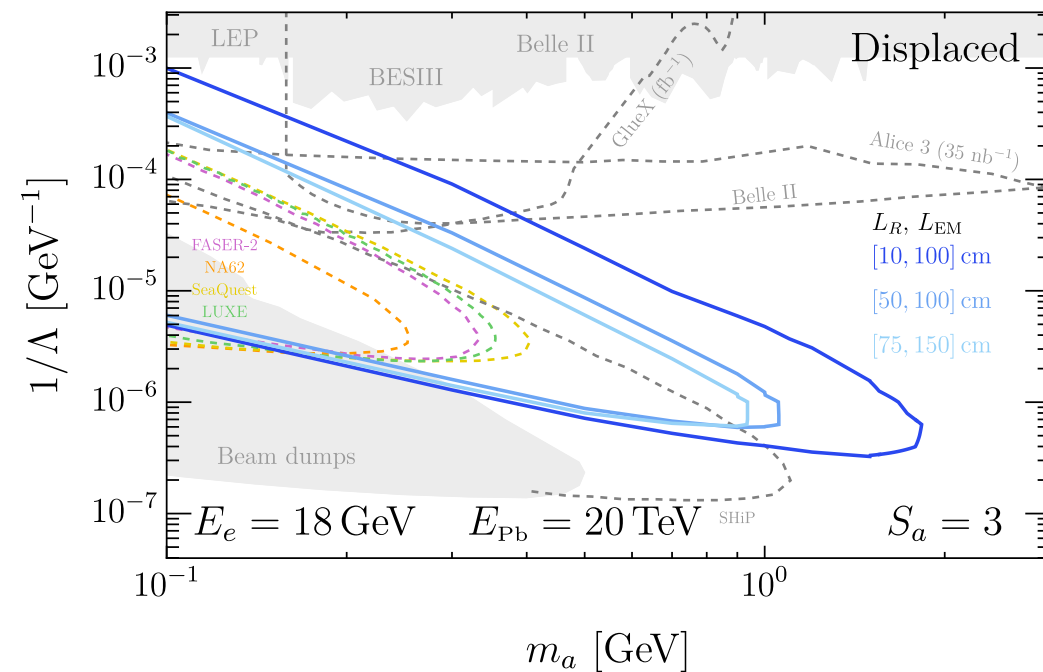
EIC projections: displaced-vertex searches

- Background free

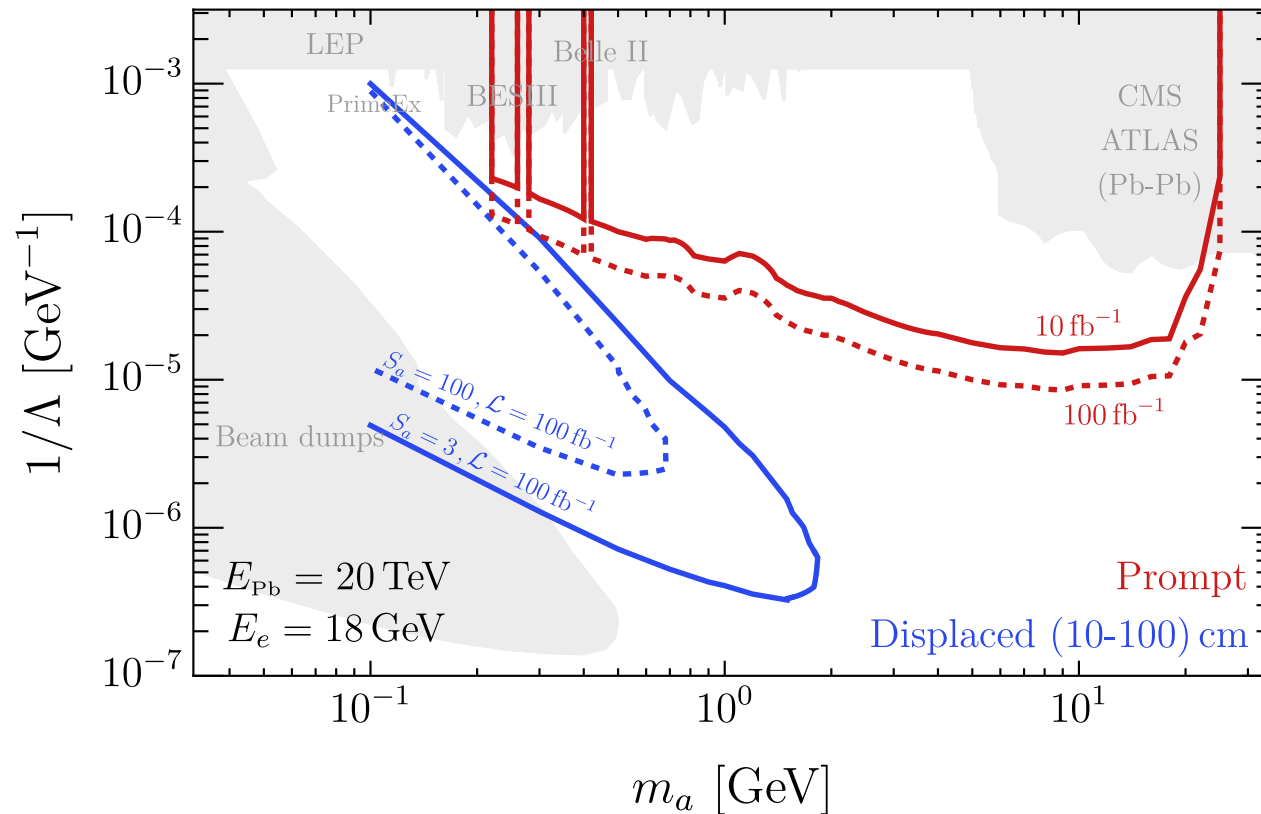
- Bounds are set by $S_a = 3$

- Flat background 2500 ($\mathcal{L}/100 \text{ fb}^{-1}$)

- Bounds are set by $S_a/\sqrt{B} = 2$



Summary



- EIC is good at detecting coherent process.
- EIC can surpass the current lepton and hadron collider and future heavy-ion projection due to the large ALPs production cross section and high luminosity.
- EIC can reach $\Lambda \sim 10^5 \text{ GeV}$ in the 2 to 20 GeV range in the prompt searches. For displaced-vertex search, it can reach $\Lambda \sim 10^7 \text{ GeV}$ for GeV ALPs.

Thanks!

Back-up slides

Merge efficiencies

[arXiv:2207.09437]

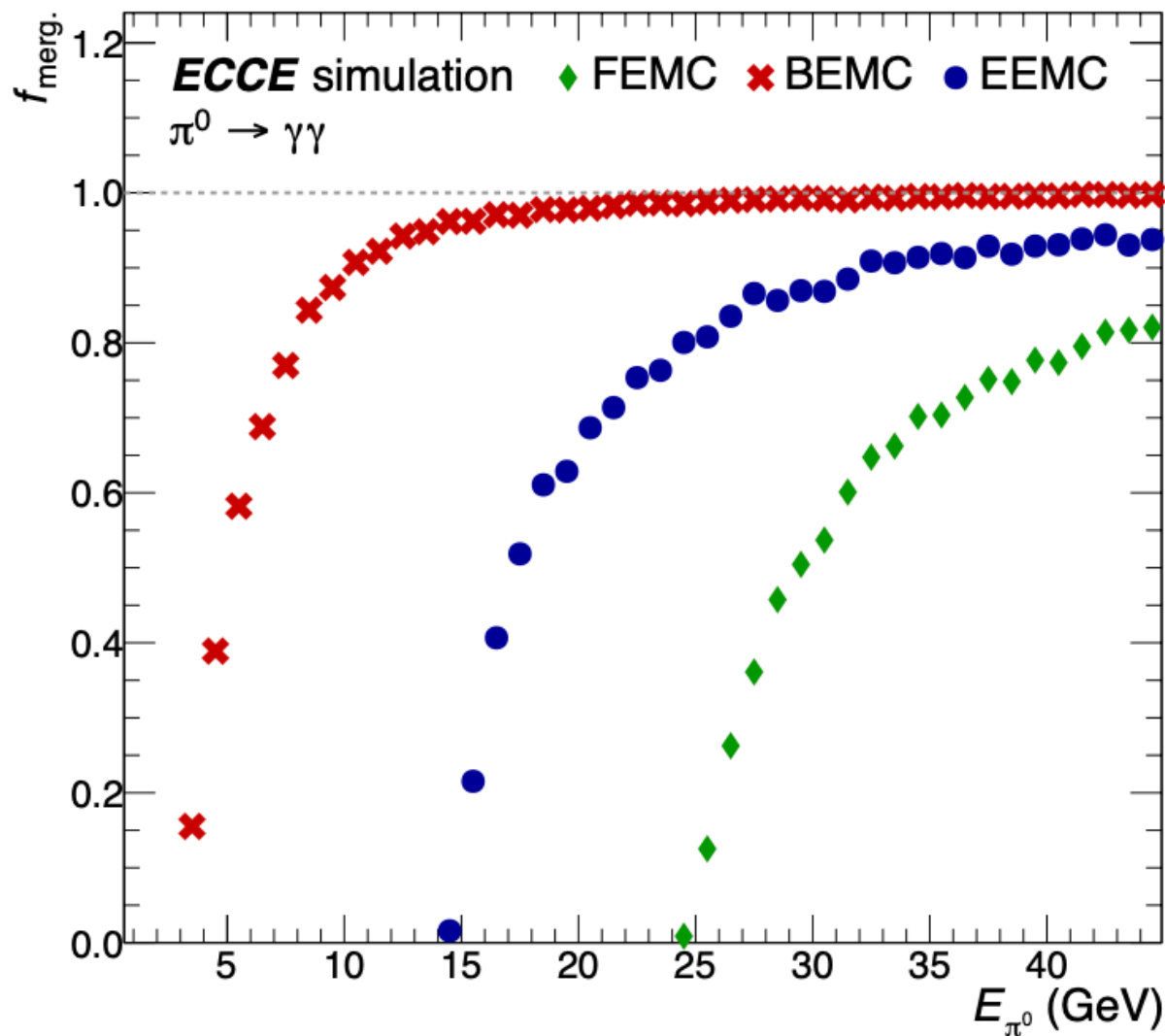


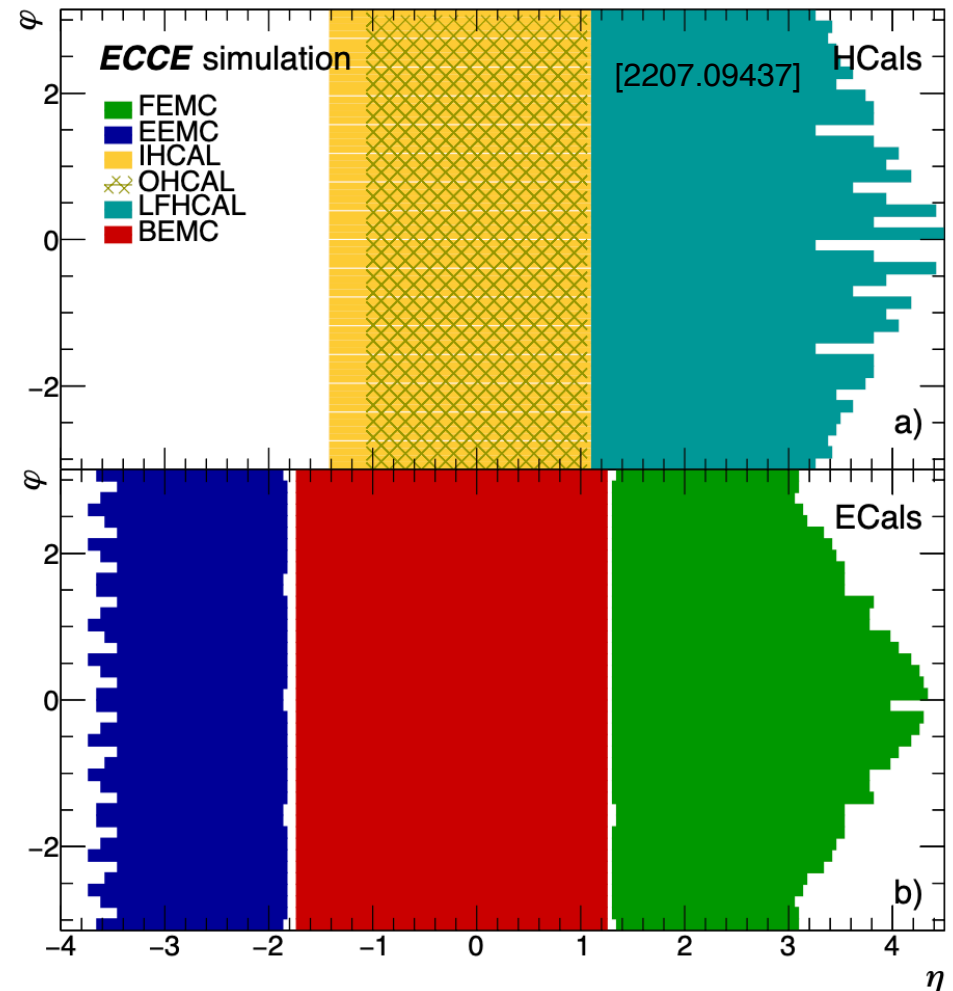
Figure 19: Fraction of neutral pions for which the showers from their decay photons are merged into a single cluster and can not be reconstructed using an invariant-mass-based approach for the different ECals.

Electron ion collider

Calorimeter	Pseudorapidity acceptance	Projected energy resolution ($\Delta E/E$) [%]
FEMC	[+1.3, +3.5]	$7.1/\sqrt{E/\text{GeV}}$
BEMC	[-1.7, +1.3]	$1.6/\sqrt{E/\text{GeV}} \oplus 0.7$
EEMC	[-3.5, -1.7]	$1.8/\sqrt{E/\text{GeV}} \oplus 0.8$

FEMC: Hadron/Forward-End-Cap Electromagnetic Calorimeter
 BEMC: Barrel Electromagnetic Calorimeter
 EEMC: Electron-End-Cap Electromagnetic Calorimeter

	EEMC	BEMC	FEMC
tower size	2x2x20 cm ³	4x4x45.5 cm ³	in: 1x1x37.5 cm ³ out: 1.6x1.6x37.5 cm ³
material	PbWO ₄	projective SciGlass	projective Pb/Scintillator
d_{abs}	-	-	1.6 mm
d_{act}	20 cm	45.5 cm	4 mm
N_{layers}	1	1	66
$N_{towers(channel)}$	2876	8960	19200/34416
X/X_0	~ 20	~ 16	~ 19
R_M	2.73 cm	3.58 cm	5.18 cm
f_{sampl}	0.914	0.970	0.220
λ/λ_0	~ 0.9	~ 1.6	~ 0.9
η acceptance	-3.7 < η < -1.8	-1.7 < η < 1.3	1.3 < η < 4
resolution			
- energy	$2/\sqrt{E} \oplus 1$	$2.5/\sqrt{E} \oplus 1.6$	$7.1/\sqrt{E} \oplus 0.3$
- φ	~ 0.03	~ 0.05	~ 0.04
- η	~ 0.015	~ 0.018	~ 0.02



[2209.02580]